ISSN 1948-0210 (online)

World Journal of *Stem Cells*

World J Stem Cells 2023 September 26; 15(9): 876-959

Published by Baishideng Publishing Group Inc

World Journal of Stem Cells

Contents

Monthly Volume 15 Number 9 September 26, 2023

ORIGINAL ARTICLE

Basic Study

876 Interferon-γ priming enhances the therapeutic effects of menstrual blood-derived stromal cells in a mouse liver ischemia-reperfusion model

Zhang Q, Zhou SN, Fu JM, Chen LJ, Fang YX, Xu ZY, Xu HK, Yuan Y, Huang YQ, Zhang N, Li YF, Xiang C

897 Mechanism of adipose-derived mesenchymal stem cell exosomes in the treatment of heart failure

Wang L, Zhang JJ, Wang SS, Li L

908 Multiomics reveal human umbilical cord mesenchymal stem cells improving acute lung injury *via* the lung-gut axis

Lv L, Cui EH, Wang B, Li LQ, Hua F, Lu HD, Chen N, Chen WY

931 Integrin beta 3-overexpressing mesenchymal stromal cells display enhanced homing and can reduce atherosclerotic plaque

Hu HJ, Xiao XR, Li T, Liu DM, Geng X, Han M, Cui W

947 Enhanced wound healing and hemostasis with exosome-loaded gelatin sponges from human umbilical cord mesenchymal stem cells

Hu XM, Wang CC, Xiao Y, Jiang P, Liu Y, Qi ZQ

World Journal of Stem Cells

Monthly Volume 15 Number 9 September 26, 2023

Contents

ABOUT COVER

Editorial Board Member of *World Journal of Stem Cells*, Khawaja Husnain Haider, PhD, Professor, Department of Basic Sciences, Sulaiman Al-Rajhi University (SRU), Al-Qaseem 52726, Saudi Arabia. kh.haider@gmail.com

AIMS AND SCOPE

The primary aim of *World Journal of Stem Cells* (*WJSC*, *World J Stem Cells*) is to provide scholars and readers from various fields of stem cells with a platform to publish high-quality basic and clinical research articles and communicate their research findings online. *WJSC* publishes articles reporting research results obtained in the field of stem cell biology and regenerative medicine, related to the wide range of stem cells including embryonic stem cells, germline stem cells, tissue-specific stem cells, adult stem cells, mesenchymal stromal cells, induced pluripotent stem cells, embryonal carcinoma stem cells, hemangioblasts, lymphoid progenitor cells, *etc*.

INDEXING/ABSTRACTING

The *WJSC* is now abstracted and indexed in Science Citation Index Expanded (SCIE, also known as SciSearch®), Journal Citation Reports/Science Edition, PubMed, PubMed Central, Scopus, Biological Abstracts, BIOSIS Previews, Reference Citation Analysis, China National Knowledge Infrastructure, China Science and Technology Journal Database, and Superstar Journals Database. The 2023 Edition of Journal Citation Reports® cites the 2022 impact factor (IF) for *WJSC* as 4.1; IF without journal self cites: 3.9; 5-year IF: 4.5; Journal Citation Indicator: 0.53; Ranking: 15 among 29 journals in cell and tissue engineering; Quartile category: Q3; Ranking: 99 among 191 journals in cell biology; and Quartile category: Q3. The *WJSC*'s CiteScore for 2022 is 8.0 and Scopus CiteScore rank 2022: Histology is 9/57; Genetics is 68/325; Genetics (clinical) is 19/90; Molecular Biology is 119/380; Cell Biology is 95/274.

RESPONSIBLE EDITORS FOR THIS ISSUE

Production Editor: *Xiang-Di Zhang*; **Production Department Director:** *Xu Guo*; **Editorial Office Director:** *Jia-Ru Fan*.

NAME OF JOURNAL
World Journal of Stem Cells

ISSN
ISSN 1948-0210 (online)

LAUNCH DATE
December 31, 2009

FREQUENCY
Monthly

EDITORS-IN-CHIEF
Shengwen Calvin Li, Carlo Ventura

EDITORIAL BOARD MEMBERS
https://www.wjgnet.com/1948-0210/editorialboard.htm

PUBLICATION DATE
September 26, 2023

COPYRIGHT
© 2023 Baishideng Publishing Group Inc

INSTRUCTIONS TO AUTHORS
https://www.wjgnet.com/bpg/gerinfo/204

GUIDELINES FOR ETHICS DOCUMENTS
https://www.wjgnet.com/bpg/GerInfo/287

GUIDELINES FOR NON-NATIVE SPEAKERS OF ENGLISH
https://www.wjgnet.com/bpg/gerinfo/240

PUBLICATION ETHICS
https://www.wjgnet.com/bpg/GerInfo/288

PUBLICATION MISCONDUCT
https://www.wjgnet.com/bpg/gerinfo/208

ARTICLE PROCESSING CHARGE
https://www.wjgnet.com/bpg/gerinfo/242

STEPS FOR SUBMITTING MANUSCRIPTS
https://www.wjgnet.com/bpg/GerInfo/239

ONLINE SUBMISSION
https://www.f6publishing.com

© 2023 Baishideng Publishing Group Inc. All rights reserved. 7041 Koll Center Parkway, Suite 160, Pleasanton, CA 94566, USA
E-mail: bpgoffice@wjgnet.com https://www.wjgnet.com

World Journal of Stem Cells

Submit a Manuscript: https://www.f6publishing.com

World J Stem Cells 2023 September 26; 15(9): 908-930

DOI: 10.4252/wjsc.v15.i9.908

ISSN 1948-0210 (online)

ORIGINAL ARTICLE

Basic Study

Multiomics reveal human umbilical cord mesenchymal stem cells improving acute lung injury *via* the lung-gut axis

Lu Lv, En-Hai Cui, Bin Wang, Li-Qin Li, Feng Hua, Hua-Dong Lu, Na Chen, Wen-Yan Chen

Specialty type: Cell and tissue engineering

Provenance and peer review: Unsolicited article; Externally peer reviewed.

Peer-review model: Single blind

Peer-review report's scientific quality classification

Grade A (Excellent): A
Grade B (Very good): B
Grade C (Good): C, C
Grade D (Fair): 0
Grade E (Poor): 0

P-Reviewer: Shamseldeen AM, Egypt; Sheykhhasan M, Iran; Sultana N, Bangladesh; Li SC, United States

Received: May 12, 2023
Peer-review started: May 12, 2023
First decision: June 29, 2023
Revised: July 23, 2023
Accepted: September 6, 2023
Article in press: September 6, 2023
Published online: September 26, 2023

Lu Lv, En-Hai Cui, Bin Wang, Feng Hua, Hua-Dong Lu, Na Chen, Wen-Yan Chen, Department of Respiratory and Critical Care Medicine, Huzhou Central Hospital, Affiliated Huzhou Hospital, Zhejiang University School of Medicine, Huzhou 313000, Zhejiang Province, China

Li-Qin Li, Traditional Chinese Medicine Key Laboratory Cultivation Base of Zhejiang Province for the Development and Clinical Transformation of Immunomodulatory Drugs, Huzhou 313000, Zhejiang Province, China

Corresponding author: En-Hai Cui, BM BCh, Doctor, Department of Respiratory and Critical Care Medicine, Huzhou Central Hospital, Affiliated Huzhou Hospital, Zhejiang University School of Medicine, No. 1558 Third Ring North Road, Huzhou 313000, Zhejiang Province, China. kjkceh@126.com

Abstract

BACKGROUND

Acute lung injury (ALI) and its final severe stage, acute respiratory distress syndrome, are associated with high morbidity and mortality rates in patients due to the lack of effective specific treatments. Gut microbiota homeostasis, including that in ALI, is important for human health. Evidence suggests that the gut microbiota improves lung injury through the lung-gut axis. Human umbilical cord mesenchymal cells (HUC-MSCs) have attractive prospects for ALI treatment. This study hypothesized that HUC-MSCs improve ALI *via* the lung-gut microflora.

AIM

To explore the effects of HUC-MSCs on lipopolysaccharide (LPS)-induced ALI in mice and the involvement of the lung-gut axis in this process.

METHODS

C57BL/6 mice were randomly divided into four groups (18 rats per group): Sham, sham + HUC-MSCs, LPS, and LPS + HUC-MSCs. ALI was induced in mice by intraperitoneal injections of LPS (10 mg/kg). After 6 h, mice were intervened with 0.5 mL phosphate buffered saline (PBS) containing 1 × 10^6 HUC-MSCs by intraperitoneal injections. For the negative control, 100 mL 0.9% NaCl and 0.5 mL PBS were used. Bronchoalveolar lavage fluid (BALF) was obtained from anesthetized mice, and their blood, lungs, ileum, and feces were obtained by an aseptic technique following CO_2 euthanasia. Wright's staining, enzyme-linked immunosorbent assay, hematoxylin-eosin staining, Evans blue dye leakage assay,

immunohistochemistry, fluorescence *in situ* hybridization, western blot, 16S rDNA sequencing, and non-targeted metabolomics were used to observe the effect of HUC-MSCs on ALI mice, and the involvement of the lung-gut axis in this process was explored. One-way analysis of variance with post-hoc Tukey's test, independent-sample Student's *t*-test, Wilcoxon rank-sum test, and Pearson correlation analysis were used for statistical analyses.

RESULTS

HUC-MSCs were observed to improve pulmonary edema and lung and ileal injury, and decrease mononuclear cell and neutrophil counts, protein concentrations in BALF and inflammatory cytokine levels in the serum, lung, and ileum of ALI mice. Especially, HUC-MSCs decreased Evans blue concentration and Toll-like receptor 4, myeloid differentiation factor 88, p-nuclear factor kappa-B (NF-κB)/NF-κB, and p-inhibitor α of NF-κB (p-IκBα)/IκBα expression levels in the lung, and raised the pulmonary vascular endothelial-cadherin, zonula occludens-1 (ZO-1), and occludin levels and ileal ZO-1, claudin-1, and occludin expression levels. HUC-MSCs improved gut and BALF microbial homeostases. The number of pathogenic bacteria decreased in the BALF of ALI mice treated with HUC-MSCs. Concurrently, the abundances of *Oscillospira* and *Coprococcus* in the feces of HUS-MSC-treated ALI mice were significantly increased. In addition, *Lactobacillus*, *Bacteroides*, and *unidentified_Rikenellaceae* genera appeared in both feces and BALF. Moreover, this study performed metabolomic analysis on the lung tissue and identified five upregulated metabolites and 11 downregulated metabolites in the LPS + MSC group compared to the LPS group, which were related to the purine metabolism and the taste transduction signaling pathways. Therefore, an intrinsic link between lung metabolite levels and BALF flora homeostasis was established.

CONCLUSION

This study suggests that HUM-MSCs attenuate ALI by redefining the gut and lung microbiota.

Key Words: Acute lung injury; Human umbilical cord mesenchymal cells; Lipopolysaccharide; Microflora; Untargeted metabolomics; Toll-like receptor 4/nuclear factor kappa-B signaling pathway

©The Author(s) 2023. Published by Baishideng Publishing Group Inc. All rights reserved.

Core Tip: The results of this study suggest that human umbilical cord mesenchymal cells (HUC-MSCs) inhibit the inflammatory cytokine expression levels in serum and the lung of mice with acute lung injury (ALI), which may be achieved by redefining the gut and lung microbiota. This study not only provides a scientific basis for the pathophysiological mechanisms and clinical application of HUC-MSCs, but it also provides new ideas for the development of therapeutic strategies for ALI.

Citation: Lv L, Cui EH, Wang B, Li LQ, Hua F, Lu HD, Chen N, Chen WY. Multiomics reveal human umbilical cord mesenchymal stem cells improving acute lung injury *via* the lung-gut axis. *World J Stem Cells* 2023; 15(9): 908-930
URL: https://www.wjgnet.com/1948-0210/full/v15/i9/908.htm
DOI: https://dx.doi.org/10.4252/wjsc.v15.i9.908

INTRODUCTION

Acute lung injury (ALI), whose final severe stage is defined as acute respiratory distress syndrome (ARDS), is caused by various pathogenic factors, including acute pneumonia, sepsis, severe trauma, and acute pancreatitis[1]. It is primarily characterized by pulmonary edema and acute inflammation[2], and has high morbidity and mortality rates in patients due to the lack of effective patient-specific treatments[3]. Therefore, ALI has received much attention from the academic community, and significant developments have been made in understanding its pathophysiological mechanisms; however, clinically available treatments for ALI are still limited[4]. Lipopolysaccharide (LPS), a common pathogenic factor associated with ALI, is the main constituent of the Gram-negative bacterial cell wall[5]. A previous study found that LPS induced lung tissue damage and increased the expression of inflammatory factors in the bronchoalveolar lavage fluid (BALF)[6]. Animal models of LPS-induced lung injury are commonly used to study ALI[7]. Interestingly, LPS-induced ALI mice have a gut microbiota imbalance, and improvement in gut microbiota homeostasis can ameliorate lung inflammation of ALI mice and inhibit Toll-like receptor 4 (TLR4)/nuclear factor kappa-B (NF-κB) signaling in the lungs [8], suggesting the possible involvement of the intestinal microbiota in ALI.

A prospective observational cohort study focused on the relationship between lung microbiota and ALI and found that BALF microbiota can predict clinical outcomes in critically ill patients, especially the enrichment of gut-associated bacteria in BALF[9]. There is increasing evidence that the effects of host-microorganism interactions extend well beyond the local environment and influence the responses of peripheral tissues[7]. Homeostasis of the gut microbiota is important for human health, including its modulatory effects on ALI[10]. A study, based on 16S rRNA amplicon and metagenomic sequencing, found that the composition of the gut microbiota has a significant impact on wasting and death

in mice with ALI, suggesting the importance of the lung-gut microbiota crosstalk in lung injury[11]. Moreover, the depletion of gut microbes using an antibiotic cocktail improves lung injury and decreases interleukin (IL)-6 levels in the BALF of ALI mice[12]. A clinical cohort study found that the gut microbiome composition in patients with coronavirus disease 2019 (COVID-19), a respiratory illness, was significantly altered compared with that in non-COVID-19 individuals, irrespective of whether patients had received medication, and that the gut microbiome composition was correlated with disease severity[13]. Additionally, intestinal diseases alter the composition of the pulmonary microbiota and their metabolites[14]. Therefore, changes in the abundance and composition of the gut microbiota may be key to improving ALI *via* the lung-gut microflora. Recently, the impact of gut microbiota homeostasis on lung diseases has come into focus.

Mesenchymal stem cells (MSCs) are multipotent cells that can differentiate into various specialized cell types, including osteoblasts, chondrocytes, and adipocytes[15]. They originate from the mesoderm and are widely derived from adult stem cells with multi-differentiation potential, and can be isolated from a variety of tissues, such as the bone marrow, umbilical cord, amniotic membrane, adipose tissue, and skeletal muscle[16]. In addition, they have been shown to have beneficial effects in ALI[17]. Human umbilical cord mesenchymal cells (HUC-MSCs) have gained popularity in stem cell research and applications because of their specific advantages, including easy availability, abundance, lack of tumorigenicity, and ethical compliance[18]. Ahn *et al*[19] found that HUC-MSCs improved chronic lung disease and bronchopulmonary dysplasia in premature infants, without any transplantation-related adverse outcomes. Additionally, HUC-MSCs improved lung injury and inhibited the pro-inflammatory cytokine levels in the lungs of LPS-induced ALI mice[20]. HUC-MSC treatment ameliorated lung inflammation and fibrosis in bleomycin-induced pulmonary fibrosis mice[21]. Furthermore, researchers have reported that intraperitoneal infusions of HUC-MSCs improve colitis by reshaping the diversification of the gut microbiota[22]. Additionally, the gut microbiota of pulmonary hypertension mice was reversed by MSC treatment[23]. Studies on the HUC-MSC treatment of inflammation-related diseases are developing rapidly; however, their mechanisms of action are poorly understood. Therefore, by analyzing the lung-gut microbiota and lung metabolomics, this study aimed to explore the mechanisms underlying the amelioration of ALI by HUC-MSCs to provide a scientific basis for the clinical application of HUC-MSCs and a direction for the development of therapeutic strategies for ALI/ARDS.

MATERIALS AND METHODS

Animals and cells

A total of 72 6-8-wk-old male C57BL/6 mice were purchased from Beijing Vital River Laboratory Animal Technology Co., Ltd. (Beijing, China) and housed in a standard specific pathogen-free environment. The mice were isolated and allowed to adapt for one week. All procedures involving animals were approved and supervised by the Animal Experimentation Ethics Committee of Zhejiang Eyong Pharmaceutical Research and Development Center. Mycoplasma free HUC-MSCs (HUM-iCell-e009) were purchased from iCell Bioscience Inc. (Shanghai, China) and cultured in a specialized medium (PriMed-iCELL-012; iCell Bioscience, China) containing supplements at 37 °C in a 5% CO_2 incubator. The purity of HUC-MSCs was assessed by flow cytometry and was typically greater than 90%. Cell identification was performed by iCell Bioscience Inc.

Animal model of ALI

The random number method was used to divide mice into four groups, namely, sham, sham + MSCs, LPS, and LPS + MSCs groups, with 18 mice in each group. The 36 randomly selected mice were intraperitoneally injected with 100 mL of LPS (10 mg/kg) to induce ALI[7], and sham mice were administered 100 mL of 0.9% NaCl as controls. After 6 h, half of the ALI mice and half of the sham mice were given 0.5 mL of phosphate buffered saline (PBS) containing HUC-MSCs (1×10^6 cells/mL) by intraperitoneal injections[24], and the other half of the ALI mice and sham mice were given 0.5 mL of 0.9% NaCl. The mice were reared under standard laboratory conditions. The experiments were carried out by expert technicians who were blinded to the animal grouping.

Sample preparation

Three days after HUC-MSC intervention in ALI mice, BALF was obtained after the mice were anesthetized with isoflurane as reported by Wu *et al*[24]. Briefly, the trachea was flushed five times with PBS *via* a 20-gauge catheter, and all liquids were collected. Subsequently, all mice were euthanized with CO_2, and the blood, lungs, ileum, and feces were obtained using aseptic techniques. The lungs (one lung was evenly divided into four) from three mice in each group were taken, weighed, and then baked in an oven at 80 °C for 48 h to determine the dry weight to calculate the ratio of wet lung weight to dry lung weight (W/D weight ratio) as reported by Li *et al*[25]. In addition, a part of the remaining lung and ileum were made into paraffin blocks separately, and the other were stored at 80 °C for further analysis. The BALF was divided into two parts for inflammation cytokine detection and 16S rDNA sequencing, respectively.

Detection of immune cells and inflammatory cytokines

The protein concentration in the BALF was measured using the BCA assay (Beyotime, China). Additionally, the cells in BALF were precipitated and resuspended, and mononuclear cells and neutrophils were counted after Wright's staining. The levels of tumor necrosis factor (TNF)-α (ml002095-1, Enzyme-linked, China), IL-1β (ml063132-1, Enzyme-linked, China), and IL-6 (ml002293-1, Enzyme-linked, China) in the serum, lungs, and ileum were measured by enzyme-linked

Table 1 Information of antibodies used in this study

Antibody	Dilution ratio	Manufacturer	Country	Cat. No.
VE-cadherin antibody	1:2000	Affinity	United States	AF6265
ZO-1 antibody	1:5000	Proteintech	United States	21773-1-AP
Occludin antibody	1:1000	Affinity	United States	DF7504
TLR4 antibody	1:2000	Affinity	United States	AF7017
Myd88 antibody	1:1000	Affinity	United States	AF5195
p-NF-κB p65 antibody	1:2000	Affinity	United States	AF2006
NF-κB p65 antibody	1:2000	Affinity	United States	AF5006
p-IκBα antibody	1:2000	Affinity	United States	AF2002
IκB antibody	1:2000	Affinity	United States	AF5002
Claudin-1 antibody	1:3000	Affinity	United States	AF0127
Anti-rabbit IgG, HRP-linked antibody	1:6000	Cell signaling technology	United States	7074
Anti-mouse IgG, HRP-linked antibody	1:6000	Cell signaling technology	United States	7076
β-actin antibody	1:10000	Affinity	United States	AF7018

VE: Vascular endothelia; ZO-1: Zonula occludens-1; TLR4: Toll-like receptor; Myd88: Myeloid differentiation factor 88; NF-κB: Nuclear factor kappa-B; IκB α: Inhibitor α of nuclear factor kappa-B; HRP: Horse radish peroxidase.

immuno sorbent assay (ELISA) according to the manufacturer's instructions.

Histopathological observation

Hematoxylin-eosin (H&E) staining was performed to observe the histopathology of the lungs and ileum. Briefly, the lungs and ileum were fixed in 10% formalin. The tissues were then placed in paraffin and sectioned, and sections were stained with H&E. The injury of lungs and ileum were scored in a blinded fashion as previously reported[26,27].

Measurement of alveolar-capillary permeability

Three mice were randomly selected from each group for the Evans blue dye leakage assay to explore the function of the lung tissue endothelial barrier as previously reported[28]. This assay was performed using 25 mg/kg of 0.5% blue dye (Sigma, United States) injected into mice *via* the tail vein 2 h before isoflurane anesthesia. After the heart of the anesthetized mice was exposed, the left ventricle was intubated and flushed with 4% normal saline. Subsequently, the mice were euthanized using CO_2. Lungs were homogenized in 2 mL PBS and treated with formamide (Sigma, United States) at 60 °C for 24 h. Finally, the concentration of Evans blue dye in the lung tissue was determined at 620 nm using a microplate reader (CMaxPlus, Molecular Devices, United States).

Immunohistochemistry

Immunohistochemistry (IHC) was performed as described by Peng *et al*[29]. Paraffin sections of lung tissue were deparaffinized, permeabilized, and blocked. The sections were then incubated at 4 °C overnight with anti-TLR4 antibody (1:100 dilution; Affinity, United States). After washing with PBS, the slides were incubated with goat anti-rabbit IgG HRP (Abcam, United States) at 37 °C for 30 min. The slides were washed again, mounted with DAPI (Vector Laboratories, Burlingame, CA), and examined using an E100 fluorescence microscope (Nikon, Japan).

Fluorescence in situ hybridization

Fluorescence *in situ* hybridization (FISH) was performed on slides of ileum and lung tissues as previously described[30], using a pan-bacteria FITC-labeled probe (EUB338) and an RNA FISH kit (Genepharma, China). After DAPI staining, the slides were visualized under an inverted fluorescence microscope (Ts2-FL; Nikon, Japan). Images were acquired using Micro-Manager and analyzed using ImageJ/FIJI software (National Institutes of Health, United States, version 1.53c).

Western blot analysis

The antibodies used for western blot (WB) are shown in Table 1. The lung and ileum tissues were homogenized in a lysis solution for the extraction of proteins. After centrifugation and supernatant collection, the samples were uniformly concentrated and denatured. Briefly, sodium dodecyl sulfate-gel electrophoresis and membrane transfer were performed for 20 μg protein per group as reported by Li *et al*[3]. The membranes were incubated with primary antibodies overnight and then with secondary antibodies for 1 h. Finally, the membranes were subjected to chemiluminescence reactions and protein levels were measured by enhanced chemiluminescence. ImageJ/FIJI software was used for semiquantitative analysis.

16S rDNA sequencing

High-throughput 16S rDNA sequencing was performed to analyze the gut and pulmonary microflora by BioDeep Co., Ltd (Suzhou, China). A sequencing library was prepared using the TruSeq Nano DNA LT Library Prep Kit of Illumina. A NovaSeq6000 system (PE250, Illumina, United States) was used for sequencing as reported by Yi *et al*[31]. Then the QIIME2 DADA2 and OmicStudio platforms[32] were used to analyze the data.

Metabolomics for lung tissue

The non-targeted metabolomics approach was performed by PANOMIX Biomedical Tech Co., Ltd. (Suzhou, China). The samples were treated with 75% methanol-chloroform (9:1) and 25% water for sonication and centrifugation to extract the metabolites. The samples (2 μL) were analyzed by liquid chromatography-mass spectrum (MS) detection with the Vanquish UHPLC System (Thermo, United States). Additionally, an Orbitrap Exploris mass spectrometer (Thermo, United States) was used for mass spectrometry analysis. After data acquisition, the Proteowizard package (v3.0.8789) and the R xcms package were used to preprocess the data. Metabolites were identified on the public databases such as the Human Metabolome Database[33], MassBank (https://massbank.eu/MassBank/), Lipid Maps (https://Lipidmaps.org/), mzCloud (https://www.mzcloud.org/), Kyoto Encyclopedia of Genes and Genomes (KEGG)[34], and self-building repository, and Orthogonal Projections to Latent Structures Discriminant Analysis (OPLS-DA) analysis was performed to screen the differential metabolites.

Statistical analysis

Statistical analyses were performed using SPSS (version 16.0; IBM, Armonk, NY, United States). Data from multiple *in vivo* experiments were analyzed using one-way analysis of variance (ANOVA) with a post-hoc Tukey test. The independent-samples Student's *t*-test was used for comparison between the two groups. The Wilcoxon rank-sum test was conducted to explore the microflora with a significant difference in abundance. Pearson's correlation analysis was used to explore the intrinsic associations. Additionally, the Variable Importance for the Projection (VIP) of OPLS-DA was used to screen for metabolites with biomarker potential (VIP > 1). Two-way Orthogonal Partial Least Squares (O2PLS) analysis was used to explore the links between BALF microbiota and lung metabolism. The threshold for significance was $P < 0.05$ for all tests.

RESULTS

HUC-MSC treatment alleviates lung injury and inflammation in ALI mice

This study used LPS to induce ALI in mice and then collected their lungs and BALF to explore the ameliorating effect of HUC-MSCs on ALI by H&E staining and ELISA. ALI mice had a higher lung W/D weight ratio and more mononuclear cells and neutrophils than sham mice ($P < 0.01$), whereas HUC-MSC treatment on ALI mice decreased the lung W/D weight ratio ($P < 0.05$), mononuclear cell and neutrophil counts, and protein concentration ($P < 0.01$) (Figures 1A and B). Additionally, compared to sham mice, the lung of ALI mice had markedly thickened alveolar septa with significant inflammatory cell infiltration; however, HUC-MSC treatment alleviated the degree of alveolar septal thickening and inflammatory cell infiltration in ALI mice (Figure 1C). Likewise, the score of lung injury in the LPS group was higher than those in the sham ($P < 0.01$) and LPS + MSC groups ($P < 0.05$) (Figure 1D). Moreover, ALI mice had significantly increased levels of TNF-α, IL-1β, and IL-6 in their serum and lung tissues ($P < 0.01$) (Figures 1E and F). In particular, the above-mentioned inflammatory factor levels were decreased in the ALI mice treated with HUC-MSCs ($P < 0.01$) (Figures 1E and F).

HUC-MSC treatment improves endothelial barrier function and integrity in the lungs of ALI mice

In addition, this study observed the endothelial barrier function and integrity of the lungs using Evans blue, WB, and IHC assays. As shown in Figure 2A, ALI mice had a higher concentration of Evans blue dye in the lungs than the sham mice, and HUC-MSC treatment reduced Evans blue concentration in the lungs of ALI mice ($P < 0.01$). In particular, the levels of endothelial barrier-associated proteins, such as vascular endothelial (VE)-cadherin, zonula occludens-1 (ZO-1), and occludin, were markedly decreased in ALI mice ($P < 0.05$ or $P < 0.01$); however, HUC-MSC treatment reversed the expression levels of these proteins ($P < 0.01$) (Figures 2B-D). In addition, this study explored the signal intensity of the TLR4/myeloid differentiation factor 88 (Myd88)/NF-κB signaling pathway. The TLR4, Myd88, p-NF-κB/NF-κB, and p-inhibitor α of NF-κB (p-IκBα)/IκBα expression levels in the lung were all increased in ALI mice compared to the sham mice ($P < 0.01$); however, in ALI mice treated with HUC-MSCs, the expression levels of these proteins were decreased ($P < 0.05$ or $P < 0.01$) (Figures 2E-I). Similarly, TLR4 detected by IHC had a strong positive expression in the lungs of ALI mice, whereas HUC-MSC treatment attenuated the positive expression of TLR4 ($P < 0.05$ or $P < 0.01$) (Figures 2J and K).

HUC-MSC treatment improves injury, endothelial barrier integrity, and bacterial translocation in the ileum of ALI mice

Studies have reported not only lung function injury but also intestinal dysfunction in ALI[17]. Therefore, the ileum was examined using H&E staining, ELISA, WB, and FISH. The ileal tissue of ALI mice had shorter and ruptured villi with significant inflammatory cell infiltration compared to sham mice, whereas these ileal injuries in ALI mice treated with HUC-MSCs were improved ($P < 0.05$ or $P < 0.01$) (Figure 3A). In addition, LPS treatment on mice markedly increased the ileal TNF-α, IL-1β, and IL-6 levels ($P < 0.01$), whereas HUC-MSC treatment inhibited them ($P < 0.01$) (Figure 3B). The suppressed expression of endothelial barrier-associated proteins, including claudin, ZO-1, and occludin by LPS was

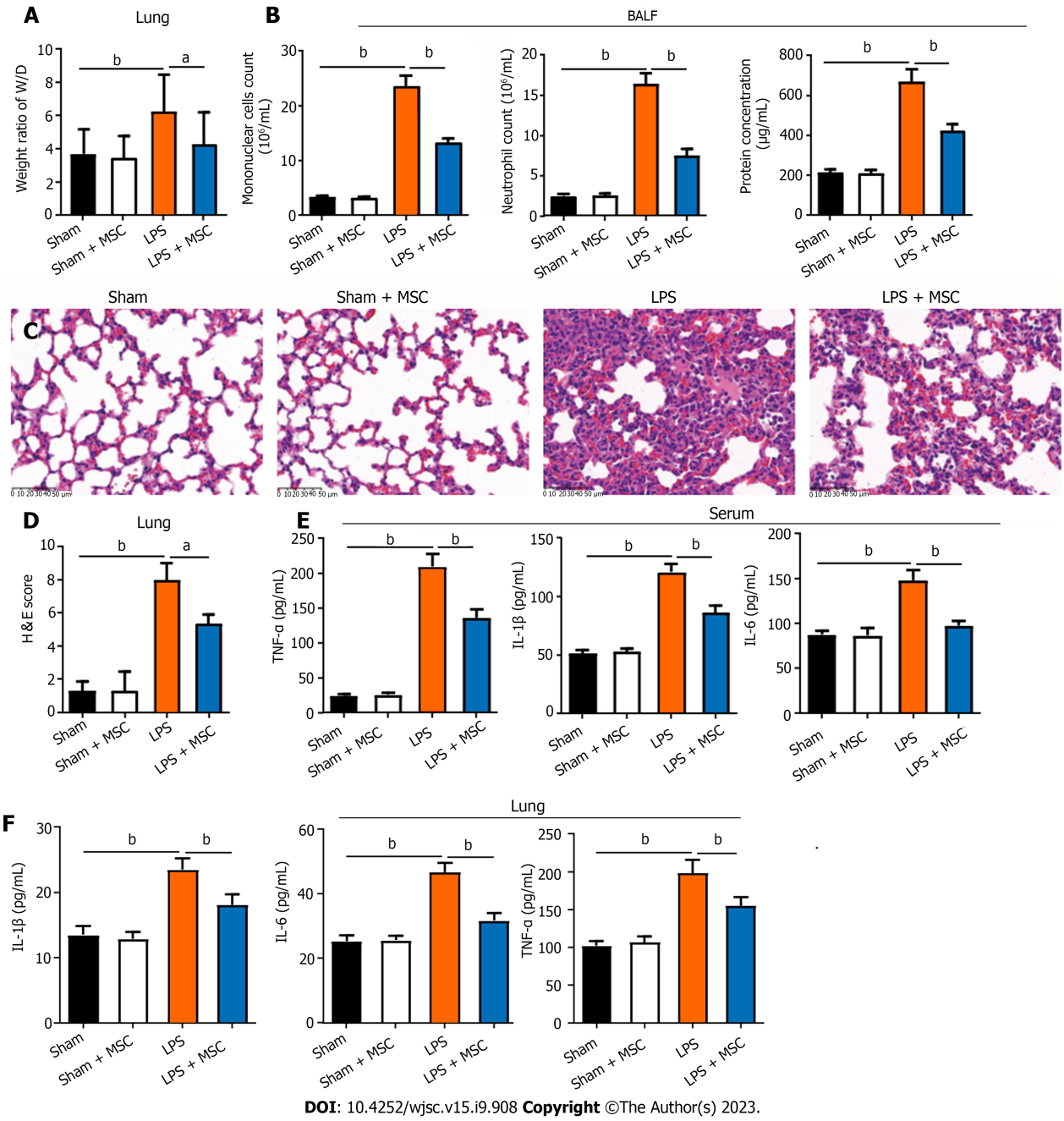

DOI: 10.4252/wjsc.v15.i9.908 **Copyright** ©The Author(s) 2023.

Figure 1 Human umbilical cord mesenchymal stem cells attenuate lipopolysaccharide-induced lung injury and inflammation in acute lung injury mice. A: In acute lung injury (ALI) mice, the wet-to-dry (W/D) weight ratio of the lung was higher than that of human umbilical cord mesenchymal stem cell (HUC-MSC)-treated ALI mice (n = 3); B: ALI mice had more mononuclear cells and neutrophils, and higher protein concentration in bronchoalveolar lavage fluid (BALF) than sham mice, while HUC-MSC treatment decreased these parameters (n = 12); C: Representative images of hematoxylin-eosin (H&E)-stained lung tissues (× 400, scale = 50 μm); D: Lung histopathological damage in mice (H&E staining; n = 3); E: Serum tumor necrosis factor (TNF)-α, interleukin (IL)-1β, IL-6, and lipopolysaccharide levels were higher in ALI mice and HUC-MSC treatment decreased their levels (n = 12); F: TNF-α, IL-1β, and IL-6 levels in the lungs of ALI mice were hugely increased than those in sham mice, while HUC-MSC treatment in ALI mice decreased them (n = 12). $^{a}P < 0.05$, $^{b}P < 0.01$. LPS: Lipopolysaccharide; MSC: Mesenchymal stem cell; BALF: Bronchoalveolar lavage fluid; H&E: Hematoxylin-eosin; IL: Interleukin; TNF: Tumor necrosis factor.

enhanced by HUC-MSC treatment in ALI mice ($P < 0.05$) (Figures 3C and D). Furthermore, the EUB338 counts of the ileum epithelium and lungs in ALI mice were measured to observe the lung translocation of gut bacteria, and it was found that they were increased in ALI mice, whereas HUC-MSC treatment reduced them ($P < 0.01$) (Figures 3E-H).

HUC-MSC treatment attenuates ALI via regulating lung-gut microbiota homeostasis

16S rDNA sequencing was used to explore the effect of the lung and gut microbiota on the HUC-MSC-mediated amelioration of ALI. BALF and fecal samples were collected for 16S rDNA sequencing. After homogenizing the sequencing depth of each group, 48 BALF and fecal samples from the four groups were identified at the genus level, with an average of 48.25 units in each group. Figures 4A and B shows the top 20 flora with the highest average abundance at the genus level. The Shannon and Simpson indices of alpha diversity reflect richness and community evenness,

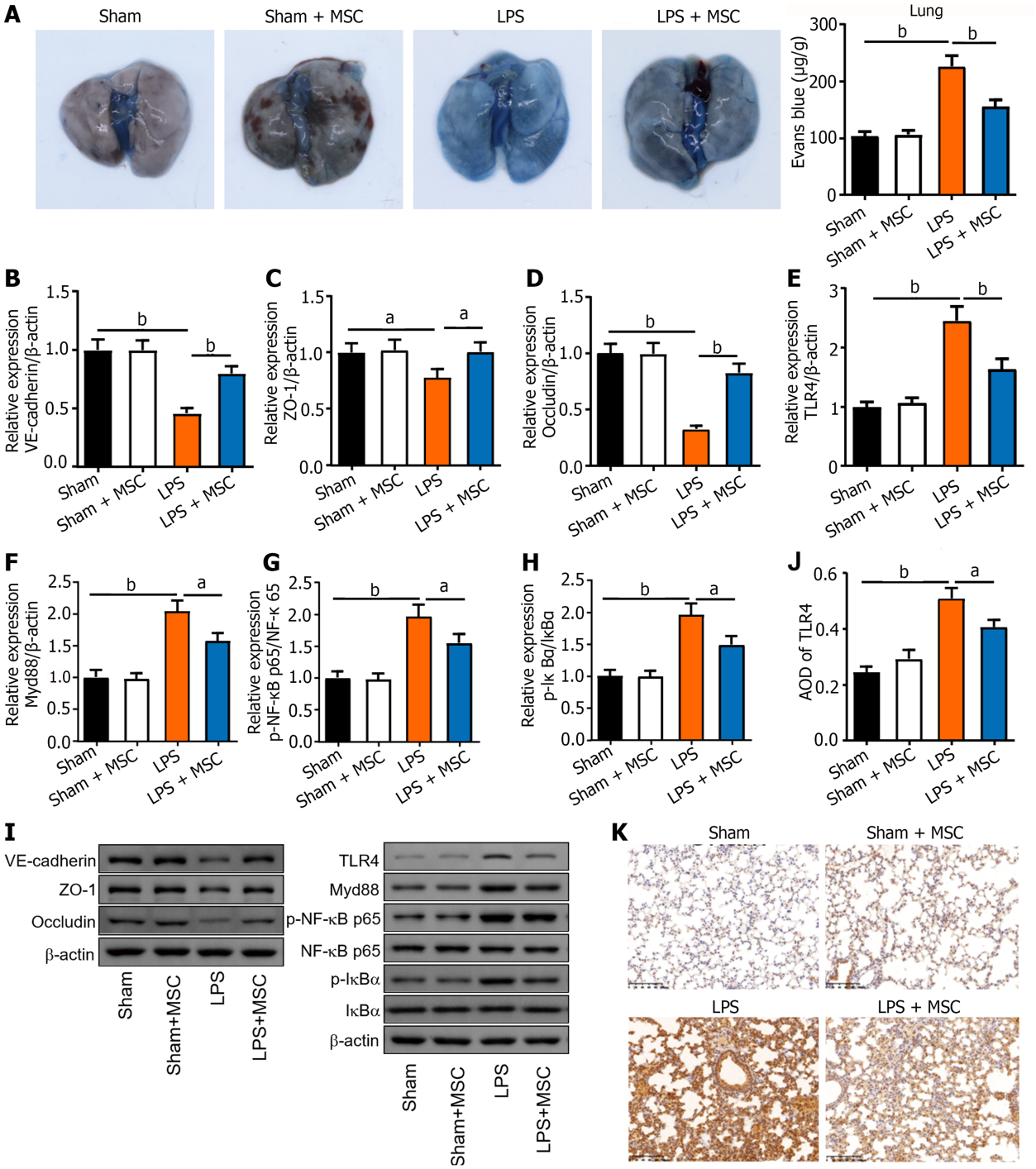

DOI: 10.4252/wjsc.v15.i9.908 **Copyright** ©The Author(s) 2023.

Figure 2 Human umbilical cord mesenchymal stem cells improve endothelial barrier function *in vivo* and regulate related protein expression. A: The Evans blue assay was carried out to assess lung endothelial barrier function in acute lung injury (ALI) mice (n = 3). The ALI mice [lipopolysaccharide (LPS) group] had the largest amount of Evans blue contents; human umbilical cord mesenchymal stem cell (HUC-MSC) treatment in ALI mice (LPS + MSC group) decreased the contents in the lung; B-H: LPS treatment in mice inhibited the expression of vascular endothelial-cadherin (B), zonula occludens-1 (C), and occludin (D) and raised the expression of Toll-like receptor 4 (TLR4) (E), myeloid differentiation factor 88 (F), p-nuclear factor kappa-B (NF-κB)/NF-κB (G), and p-inhibitor α of NF-κB (IκBα)/IκBα (H) (n = 3), while HUC-MSC treatment antagonized the effects of LPS; I: Representative western blot bands of the above proteins; J and K: Statistical results of immunohistochemistry and its representative images. It was showed that TLR4 was highly expressed in the lung tissue of ALI mice and HUC-MSC treatment could decrease its expression (n = 3). $^{a}P < 0.05$, $^{b}P < 0.01$. LPS: Lipopolysaccharide; MSC: Mesenchymal stem cell; LPS: Lipopolysaccharide; VE: Vascular endothelial; ZO-1: Zonula occludens-1; TLR4: Toll-like receptor 4; Myd88: Myeloid differentiation factor 88; NF-κB: Nuclear factor kappa-B; IκBα: Inhibitor α of nuclear factor kappa-B.

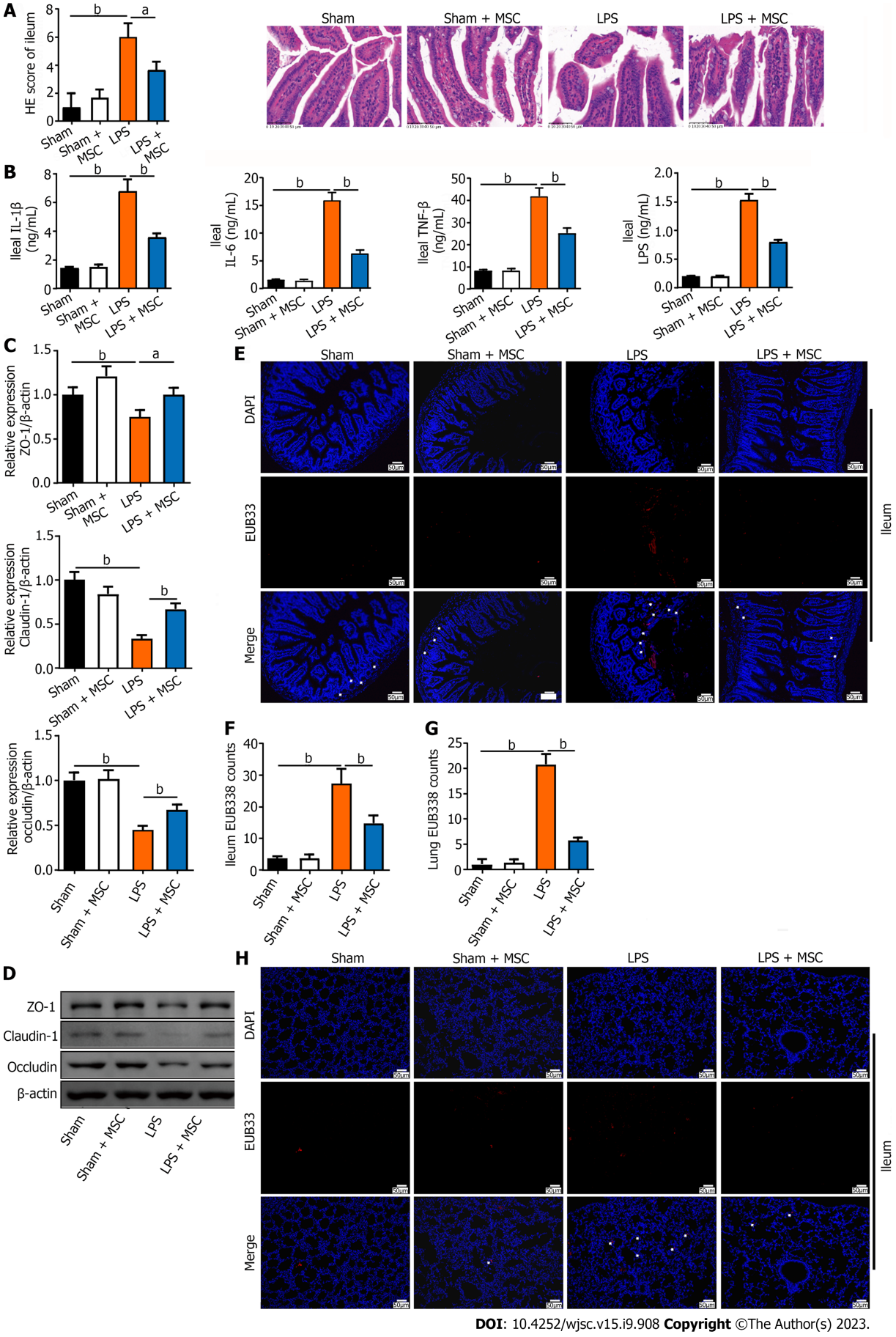

DOI: 10.4252/wjsc.v15.i9.908 **Copyright** ©The Author(s) 2023.

Figure 3 Human umbilical cord mesenchymal stem cells improve histopathology, inflammation, and endothelial barrier integrity of the

ileum in acute lung injury mice. A: Ileum tissue injury in acute lung injury (ALI) mice was observed after hematoxylin-eosin staining. ALI mice had severe ileum tissue injury while human umbilical cord mesenchymal stem cell (HUC-MSC) treatment improved such injury (n = 3); B: Tumor necrosis factor (TNF)-α, interleukin (IL)-1β, IL-6, and lipopolysaccharide (LPS) levels in the ileum were measured by ELISA (n = 12), and ALI mice had higher levels of TNF-α, IL-1β, IL-6, and LPS compared to sham mice, while HUC-MSC treatment decreased the levels of these factors; C: Zonula occludens-1 (ZO-1), claudin-1, and occludin levels were measured to observe the integrity of the ileum barrier (n = 3); D: Representative western blot bands of ZO-1, claudin-1, and occludin; E-H: Bacterial translocation was determined by fluorescence *in situ* hybridization, and the EUB338 counts in the ileum epithelium and lung per field were quantified (n = 3). $^{a}P < 0.05$, $^{b}P < 0.01$. MSC: Mesenchymal stem cell; LPS: Lipopolysaccharide; ZO-1: Zonula occludens-1; HE: Hematoxylin-eosin; IL: Interleukin; TNF: Tumor necrosis factor.

respectively. According to the Kruskal-Wallis rank-sum test, the Shannon index showed no significant differences among the groups (P = 0.056) (Figure 4C). Additionally, the Bray-Curtis distance of beta diversity reflects microbial diversity between groups and was analyzed by principal coordinates analysis, which revealed that the projection distance of the LPS + MSC group on the coordinate axis was closer to that of the negative control group than that of the LPS group (Figure 4C). Similarly, the Simpson index showed no significant differences among the groups (P = 0.058), and the projection distance of the gut microflora was closer to that of the negative control group than to that of the LPS group (Figure 4D).

Subsequently, the Wilcoxon rank-sum test was performed to explore the microflora with a significant difference in abundance (marked microflorae) (Figures 4E and F). In particular, there were 21 microflorae with upregulated abundance and 12 microflorae with downregulated abundance in the BALF of mice in the LPS + MSC group compared to the LPS group ($P < 0.05$) (Figure 4E), and 17 microflorae with upregulated abundance and 3 microflorae with downregulated abundance in feces ($P < 0.05$) (Figure 4F). The 33 marked microflorae with the largest upregulation or downregulation of operational taxonomic units in the BALF of ALI mice with/without HUC-MSC treatment are shown in Figure 5A, and 20 marked microflorae in feces are shown in Figure 5B. *Rhizobiales* had the largest log2 fold change (FC) in the BALF of mice in the LPS + MSC group compared to the LPS group [log2(FC) = 9.3264, P = 0.0284], and *Elizabethkingia* had the lowest log2FC in the BALF of mice in the LPS + MSC group compared to that of the LPS group [log2(FC) = -5.1799, P = 0.028] (Figure 5A). In fecal samples, the log2FC of *unclassified_Bacteroidales* was the highest in the marked microflorae of the LPS + MSC group compared to that of the LPS group [log2(FC) = 4.7549, P = 0.027], and that of the unidentified_F16 was the lowest [log2(FC) = -4.6328, P = 0.012] (Figure 5B).

Furthermore, the Pearson's correlation analysis was used to analyze the correlation between marked microflorae of the gut and lungs, and most of the bacteria in the BALF and feces had a strong or extremely strong correlation (Figure 6). The *Desulfovibrio* genus in feces was positively correlated with *Stenotrophomonas* in BALF ($P < 0.05$) (Supplementary Table 1).

HUC-MSC treatment regulates metabolic profile of lung tissue in ALI mice

The base peak chromatograms in the positive and negative modes of the four groups showed similar trends, suggesting good repeatability and reliable results (Figure 7A). Additionally, Partial Least Squares-Discriminant Analysis (PLS-DA) was used to distinguish metabolite differences between groups in the positive/negative mode. In particular, all blue Q2 positions in the permutation test chart were lower than the original points on the far right, suggesting that the PLS-DA models were valid (Figures 7B and C). In the positive mode, MS analysis identified a total of 1206 common biomarkers between the sham and LPS + MSC groups, 362 between the LPS and sham + MSC groups, 347 between the LPS and sham groups, 343 between the LPS + MSC and LPS groups, and 181 between the sham + MSC and sham groups (Figure 7D). In the negative mode, this study identified 905 common biomarkers between the sham and LPS + MSC groups, 476 between the LPS and sham + MSC groups, 225 between the LPS and sham groups, 112 between the LPS + MSC and LPS groups, and 139 between the sham + MSC and sham groups (Figure 7E).

Subsequently, precise screening of the metabolic profiles by MS/MS was performed to eliminate false positives. This study identified four upregulated metabolites (3-succinoylpyridine, nicotinamide ribotide, aldosterone, and phenylacetic acid) and one downregulated metabolite (lithocholic acid) in the sham + MSC group compared to the sham group. In addition, KEGG enrichment analysis suggested that these differential metabolites might participate in nicotinate and nicotinamide metabolism, aldosterone-regulated sodium reabsorption, and aldosterone synthesis and secretion pathways (Figures 8A-C). Additionally, 12 markedly upregulated metabolites (hydroxyindole, xanthine, and N-acetyl-L-aspartic acid, *etc.*) and 20 markedly downregulated metabolites (prostaglandin E2, argininosuccinic acid, and guanine, *etc.*) were identified in the LPS group compared to the sham group, and these metabolites were predicted to be potentially involved in alanine, aspartate, and glutamate metabolism, oxidative phosphorylation, the cAMP signaling pathway, and so on (Figures 8A, D and E). In particular, five upregulated metabolites (anabasine, IMP, lidocaine, salicylic acid, and propionylcarnitine) and 11 downregulated metabolites (N-acetylleucine, guanosine, guanine, *etc.*) were identified in the LPS + MSC group compared to the LPS group (Figures 8A and F). They were related to purine metabolism and the taste signaling transduction pathways ($P < 0.001$) (Figure 8G).

Significant correlations between microbes in BALF and metabolites in lung tissue

To explore the role of HUC-MSCs in regulating the microflora of the lung-gut axis to improve ALI, we performed an O2PLS correlation analysis on the expression of microflora in BALF and the expression of metabolites in the lungs to determine the microflora involved in the improvement of ALI by HUC-MSCs and their impact on metabolism. In Figure 9A, the top 25 bacteria and top 25 metabolites are shown with large absolute joint loading values, suggesting that they have a large weight in the improvement of ALI following HUC-MSC treatment. Subsequently, these flora and metabolites were analyzed using correlation analysis (Supplementary Table 1). Significantly related bacteria and metabolites were screened based on $P < 0.05$. The number of metabolites that significantly correlated with BALF microbes

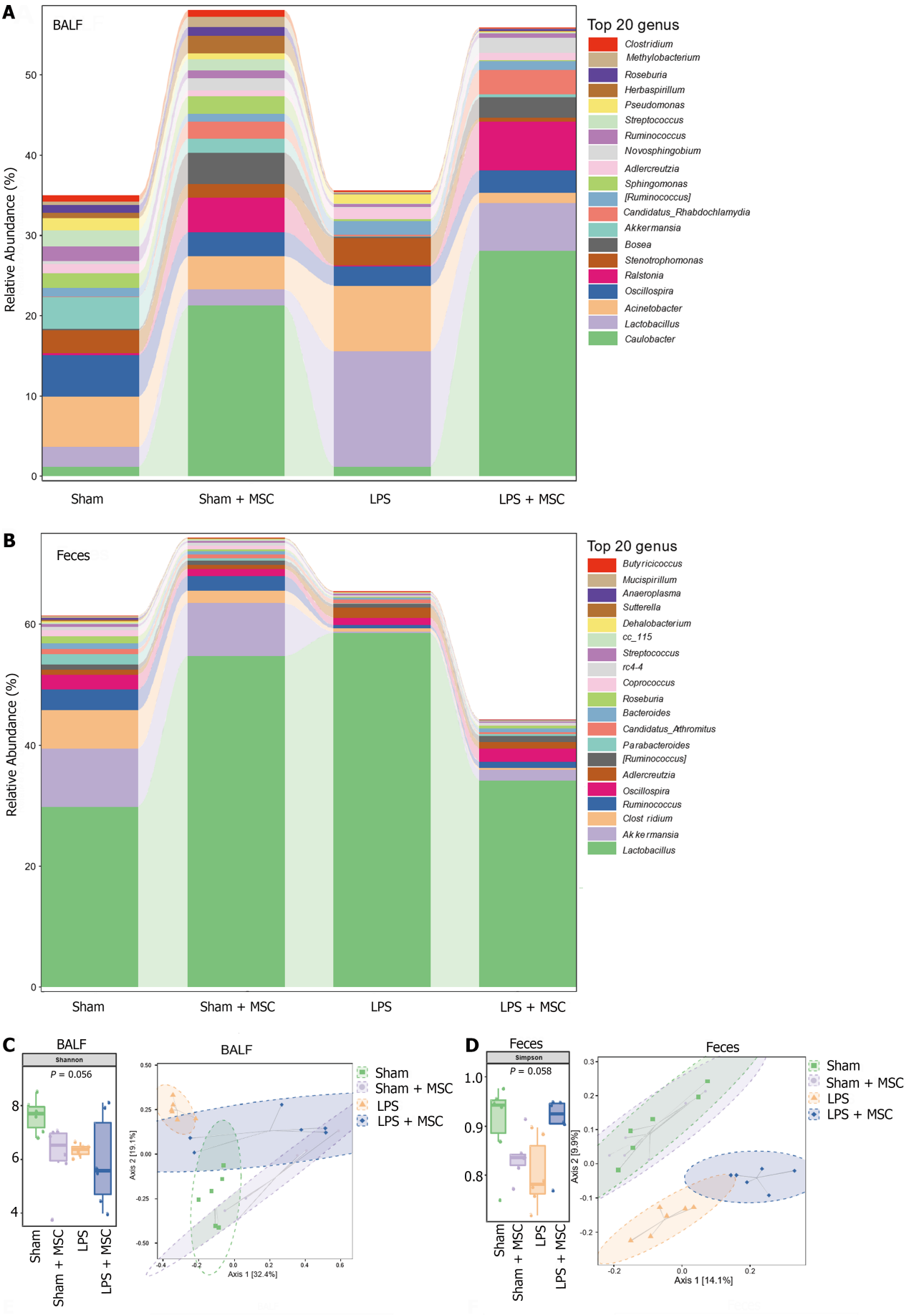
A
BALF
Relative Abundance (%)
Sham
Sham + MSC
LPS
LPS + MSC
Top 20 genus
Clostridium
Methylobacterium
Roseburia
Herbaspirillum
Pseudomonas
Streptococcus
Ruminococcus
Novosphingobium
Adlercreutzia
Sphingomonas
[Ruminococcus]
Candidatus_Rhabdochlamydia
Akkermansia
Bosea
Stenotrophomonas
Ralstonia
Oscillospira
Acinetobacter
Lactobacillus
Caulobacter
B
Feces
Relative Abundance (%)
Sham
Sham + MSC
LPS
LPS + MSC
Top 20 genus
Butyricicoccus
Mucispirillum
Anaeroplasma
Sutterella
Dehalobacterium
cc_115
Streptococcus
rc4-4
Coprococcus
Roseburia
Bacteroides
Candidatus_Athromitus
Parabacteroides
[Ruminococcus]
Adlercreutzia
Oscillospira
Ruminococcus
Clost ridium
Ak ke rmansia
Lactobacillus
C
BALF
Shannon
P = 0.056
Sham
Sham + MSC
LPS
LPS + MSC
BALF
Axis 2 [19.1%]
Axis 1 [32.4%]
Sham
Sham + MSC
LPS
LPS + MSC
D
Feces
Simpson
P = 0.058
Sham
Sham + MSC
LPS
LPS + MSC
Feces
Axis 2 [9.9%]
Axis 1 [14.1%]
Sham
Sham + MSC
LPS
LPS + MSC

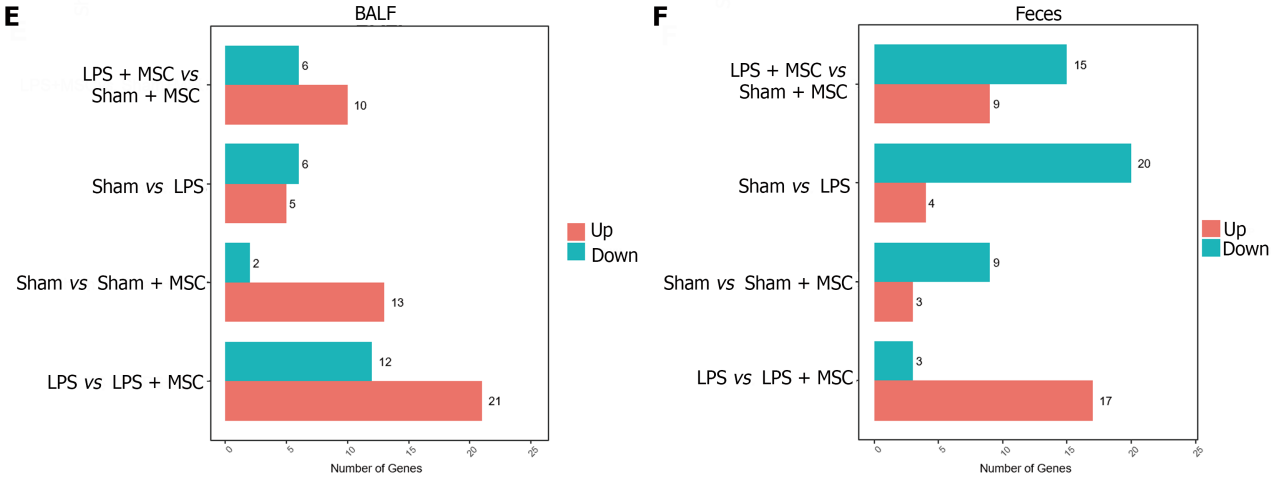

DOI: 10.4252/wjsc.v15.i9.908 **Copyright** ©The Author(s) 2023.

Figure 4 Microflora homeostasis in bronchoalveolar lavage fluid and feces of acute lung injury mice (*n* = 6). A and B: Relative abundance of top 20 genera of microflora in bronchoalveolar lavage fluid (BALF) and feces; C and D: The within-sample richness and evenness (alpha diversity) were statistically analyzed by Shannon index, Simpson index, and the bray-Curtis based principal coordinates analysis of similarity coefficients in the BALF and feces of different groups (beta diversity); E and F: The Wilcoxon rank sum test was used to explore microflorae with a significant difference in abundance on OmicShare Tools. The number of differential microflorae in lipopolysaccharide (LPS) + mesenchymal stem cells (MSCs) group *vs* sham + MSC group, sham group *vs* LPS group, sham group *vs* sham + MSC group, and LPS group *vs* LPS + MSCs group is presented. The length of the red bar indicates the number of up-regulated microflorae and the length of the blue-green bar indicates the number of down-regulated microflorae. LPS: Lipopolysaccharide; MSC: Mesenchymal stem cell; BALF: Bronchoalveolar lavage fluid.

is shown in Figure 9B. Additionally, metabolites with a large role in the improvement of ALI by HUC-MSC treatment were subjected to KEGG enrichment analysis and were found to be mainly involved in the signaling pathways of drug metabolism-other enzymes, tyrosine metabolism, autophagy-animal, and endocytosis (Figure 9C).

DISCUSSION

MSCs have emerged as a promising therapeutic strategy for inflammatory diseases, owing to their low immunogenicity, ability to stabilize immunity, and ability to ameliorate inflammatory responses[35]. Moreover, HUC-MSCs not only ameliorate acute and chronic pneumonia, but also enteritis[36,37]. This study found that HUC-MSCs improved pulmonary edema, alleviated pathological damage to the lungs and ileum, and inhibited the levels of inflammatory cells in the BALF and inflammatory factors in the serum, BALF, lungs, and ileum. Furthermore, HUC-MSC treatment of ALI mice improved endothelial barrier integrity in the lungs and ileum. Endothelial permeability is regulated by intercellular junctions including adherens junctions and tight junctions, which are composed of cell junction proteins including occludin, claudin 1, VE-cadherin, *etc*[38]. Claudin-1 in the ileum and VE-cadherin, ZO-1, and occludin in the lung and ileum play key roles in maintaining vascular integrity. This decrease indicated endothelial barrier disruption in the lungs and ileum. In this study, HUC-MSC treatment of ALI mice advanced lung VE-cadherin, ZO-1, and occludin expression signal intensity and upregulated claudin-1, ZO-1, and occludin expression levels in the ileum. Collectively, treatment of ALI mice with HUC-MSCs ameliorates lung and ileal barrier integrity.

Inflammatory factors and cells promote ALI injury. A study reported that TNF-α could promote M1 macrophage activation which has pro-inflammatory effects in sepsis-related ALI[39]. Neutrophil overactivation promotes the development of inflammation and injury in ALI[40]. Microvascular endothelial barrier dysfunction, the main pathophysiological feature of ARDS/ALI, induces capillary leakage and edema, which further intensifies inflammatory injury, thus causing high morbidity and mortality[41]. Botros and colleagues reported that stabilizing the endothelial barrier during inflammation alleviated inflammatory responses, edema, and lung injury in mice with ALI[42]. Interestingly, the inhibition of the TLR4 signaling pathways is related to the integrity of the pulmonary endothelial barrier. One study found that TLR4 knockdown decreased the sensitivity to particulate matter-induced pulmonary edema in ALI mice and increased the signal expression intensity of VE-cadherin[43]. Furthermore, MSC treatment in paraquat-induced ALI rats downregulated the TLR4 and NF-κB protein levels in the lungs[44]. Besides, LPS facilitates TLR4 activation to recruit MyD88 and thereby activates NF-κB to promote the production of pro-inflammatory factors such as TNF-α and IL-6[45]. Similarly, this study reported the inhibitory effect of HUC-MSCs on TLR4, Myd88, and NF-κB in the lungs of LPS-induced ALI mice, which suggests that HUC-MSCs may mitigate microvascular endothelial barrier dysfunction and inflammation in ALI *via* the TLR4/Myd88/NF-κB signaling pathway.

There is a correlation between microbiota levels and lung diseases[46]. By analyzing the 16S rDNA of microflora in BALF, we observed a decrease in some pathogenic bacteria. For example, the *Stenotrophomonas* genus was decreased in the BALF of mice in the LPS + MSC group. One study has reported that *Stenotrophomonas* maltophilia is commonly found

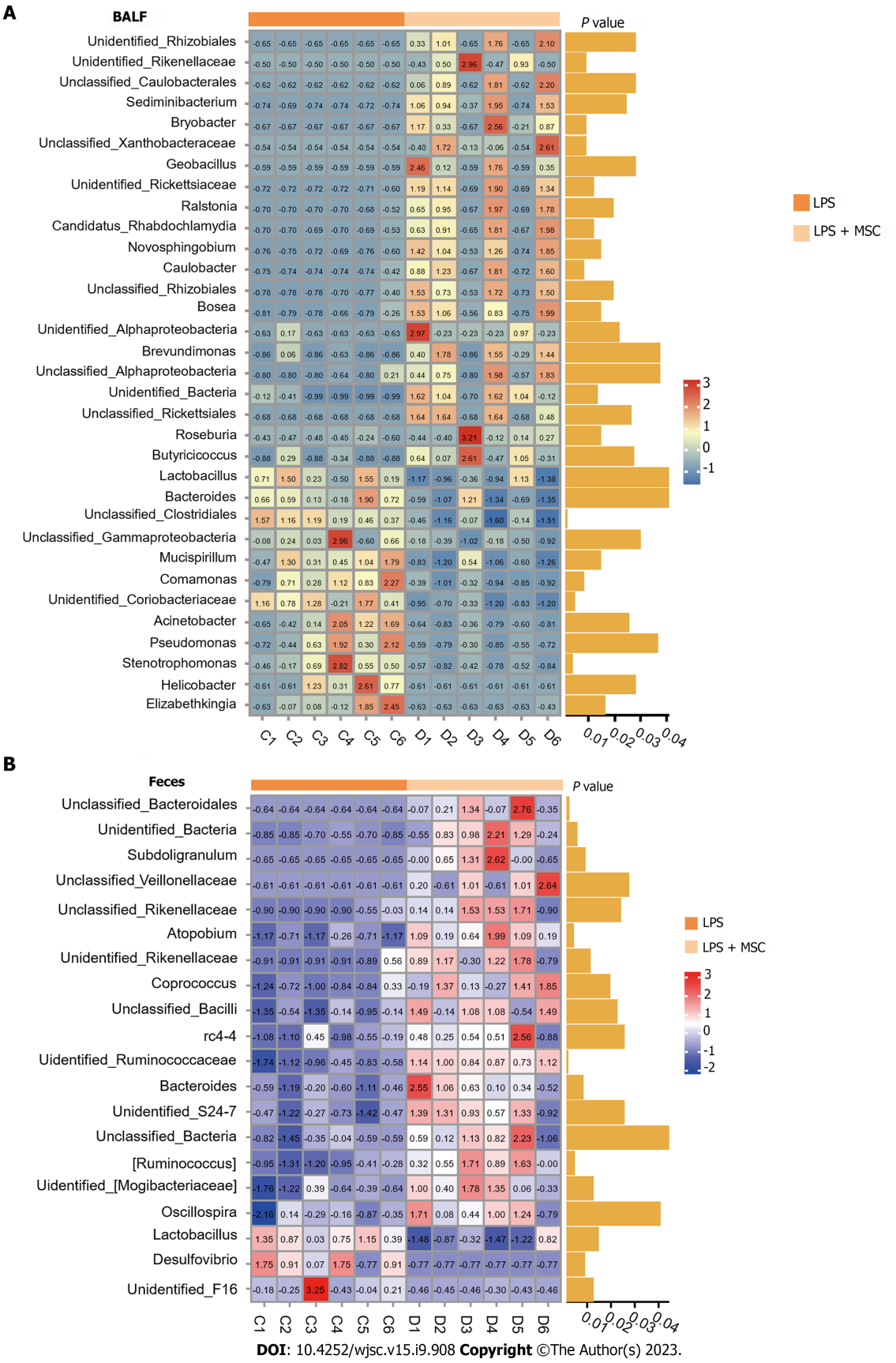

DOI: 10.4252/wjsc.v15.i9.908 **Copyright** ©The Author(s) 2023.

Figure 5 Differences in genus abundance of different microflorae in bronchoalveolar lavage fluid and feces of acute lung injury mice treated with human umbilical cord mesenchymal stem cells (*n* = 6). A and B: Heatmaps showing the differences in the genus abundance of different microflorae in bronchoalveolar lavage fluid and feces. Red represents the genus that is more highly abundant; blue/purple represents the genus that is less abundant; white/yellow indicates no difference in expression between groups. Abundance is homogenized by Z-score. The value displayed in the middle of the grid is log2 (fold change). LPS: Lipopolysaccharide; MSC: Mesenchymal stem cell; BALF: Bronchoalveolar lavage fluid.

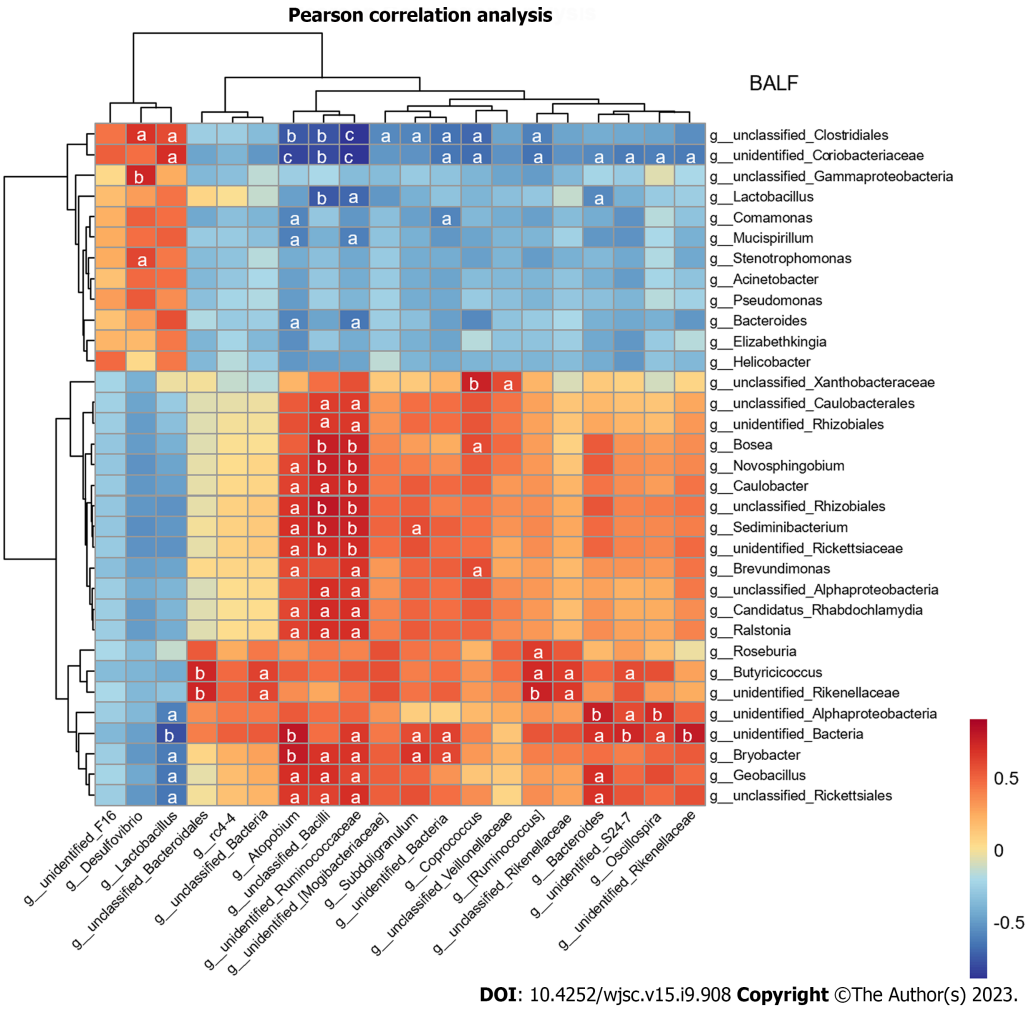

DOI: 10.4252/wjsc.v15.i9.908 **Copyright** ©The Author(s) 2023.

Figure 6 Correlation analysis between gut and lung microflorae. Person correlation analysis was used to analyze the correlation between marked microflorae of the gut and lung with OmicsStudio Tools. Red indicates positive correlation and blue indicates negative correlation. $^{a}P < 0.05$, $^{b}P < 0.01$, and $^{c}P < 0.001$ *vs* lipopolysaccharide group. BALF: Bronchoalveolar lavage fluid.

in respiratory tract infections[47]. Additionally, the *Comamonas* genus is an important opportunistic pathogen in human [48]. The genus *Elizabethkingia* has recently emerged as the cause of life-threatening infections in humans, most commonly causing meningitis[49]. *Acinetobacter Baumannii* infections have also been linked to ventilator-associated pneumonia[50]. These findings suggest that HUC-MSCs ameliorate ALI by inhibiting the abundance of pathogenic bacteria. Additionally, by analyzing the microflora in the feces, *Oscillospira* and *Coprococcus* genus abundance in the LPS + MSC group was increased. *Oscillospira*, a common genus of gut bacteria, positively correlates with gut microbiota diversity[51]. Moreover, butyrate, a product of the *Coprococcus* genus, is thought to be able to participate in anti-inflammatory processes[52]. Thus, *Oscillospira* and *Coprococcus* may be involved in the restorative effects of HUC-MSC treatment on gut microflora homeostasis. Additionally, some bacteria have contradictory roles in various diseases. The *Mucispirillum* genus is associated with Crohn's disease-like colitis in immunodeficient mice and is linked to health promotion in immunocompetent hosts[53]. In this study, the improvements in ALI may have been correlated with the abundance of microflora.

Correlation analysis of the gut and lung microflora noticed that the *Desulfovibrio* genus was positively correlated with *Stenotrophomonas*. The *Desulfovibrio* genus is a candidate microbe that induces weight loss of mice with ALI and is directly related to survival[11]. This study not only noted bacteria that strongly correlated with the downregulation of pathogenic bacterial abundance in BALF but also those that were present in both the gut and lungs. *Lactobacillus, Bacteroides,* and *unidentified_Rikenellaceae* genera appeared in the feces and BALF. Moreover, the *Bacteroides* in feces were significantly related to *Lactobacillus* in the BALF. Significant changes in their abundance may be associated with the mechanism of the lung-gut axis. Although the *Lactobacillus* genus is a beneficial flora most of the time in colitis[54], *Lactobacillus rhamnosus* GG treatment in patients with severe pneumonia does not improve the clinical outcomes[55], suggesting that changes in the abundance of *Lactobacillus* may be a consequence of the improvement of ALI by HUM-MSCs and could be used as biomarkers. *Lactobacillus, Bacteroides,* and *unidentified_Rikenellaceae* genera are potential biomarkers for evaluating the treatment efficacy of HUC-MSCs.

Moreover, lung tissue metabolomics was performed in this study, and the composition of metabolites was different in sham mice and ALI mice; HUM-MSC treatment in ALI mice changed the lung metabolite composition. The results of the metabolomic analysis suggest that HUM-MSC treatment alters the bile secretion pathway. Bile and its nuclear receptor farnesoid X are involved in inflammatory liver and bowel diseases[56]. In addition, this study verified the correlation

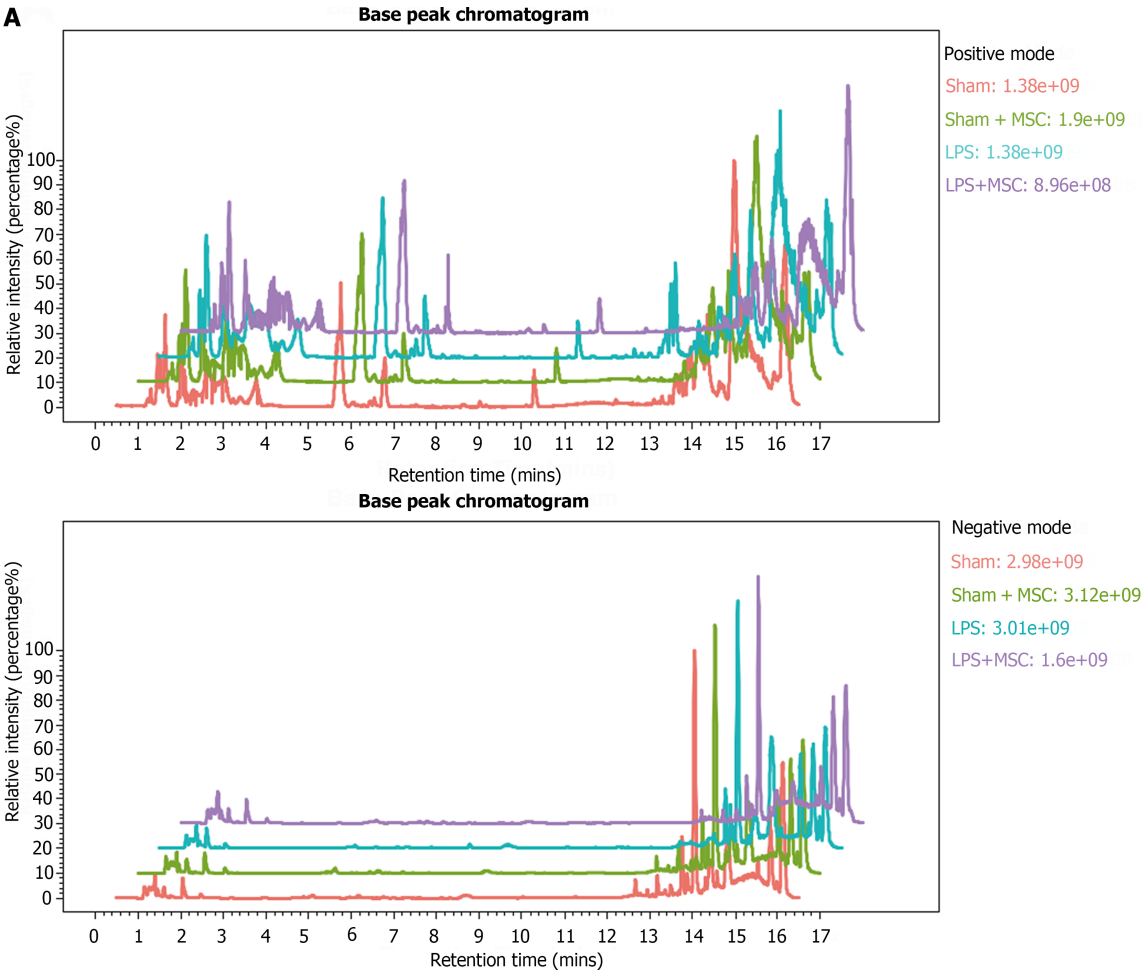
A
Base peak chromatogram
Relative intensity (percentage%)
Retention time (mins)
Positive mode
Sham: 1.38e+09
Sham + MSC: 1.9e+09
LPS: 1.38e+09
LPS+MSC: 8.96e+08
Base peak chromatogram
Relative intensity (percentage%)
Retention time (mins)
Negative mode
Sham: 2.98e+09
Sham + MSC: 3.12e+09
LPS: 3.01e+09
LPS+MSC: 1.6e+09

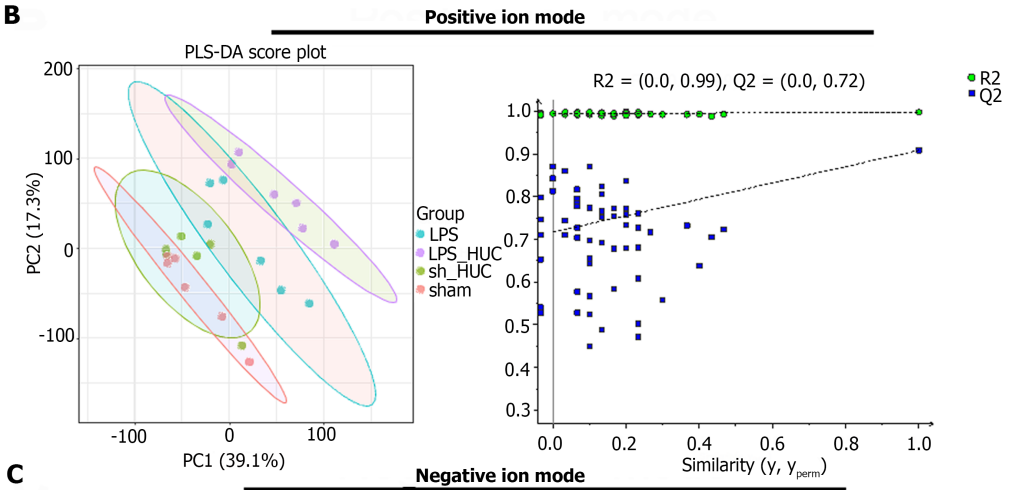
B
Positive ion mode
PLS-DA score plot
PC2 (17.3%)
PC1 (39.1%)
Group
LPS
LPS_HUC
sh_HUC
sham
R2 = (0.0, 0.99), Q2 = (0.0, 0.72)
R2
Q2
Similarity (y, y_perm)

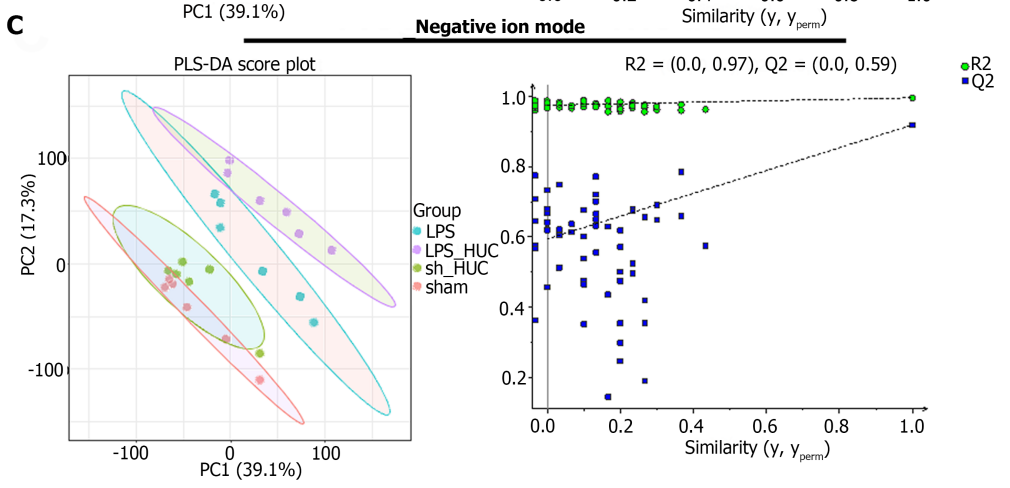
C
Negative ion mode
PLS-DA score plot
PC2 (17.3%)
PC1 (39.1%)
Group
LPS
LPS_HUC
sh_HUC
sham
R2 = (0.0, 0.97), Q2 = (0.0, 0.59)
R2
Q2
Similarity (y, y_perm)

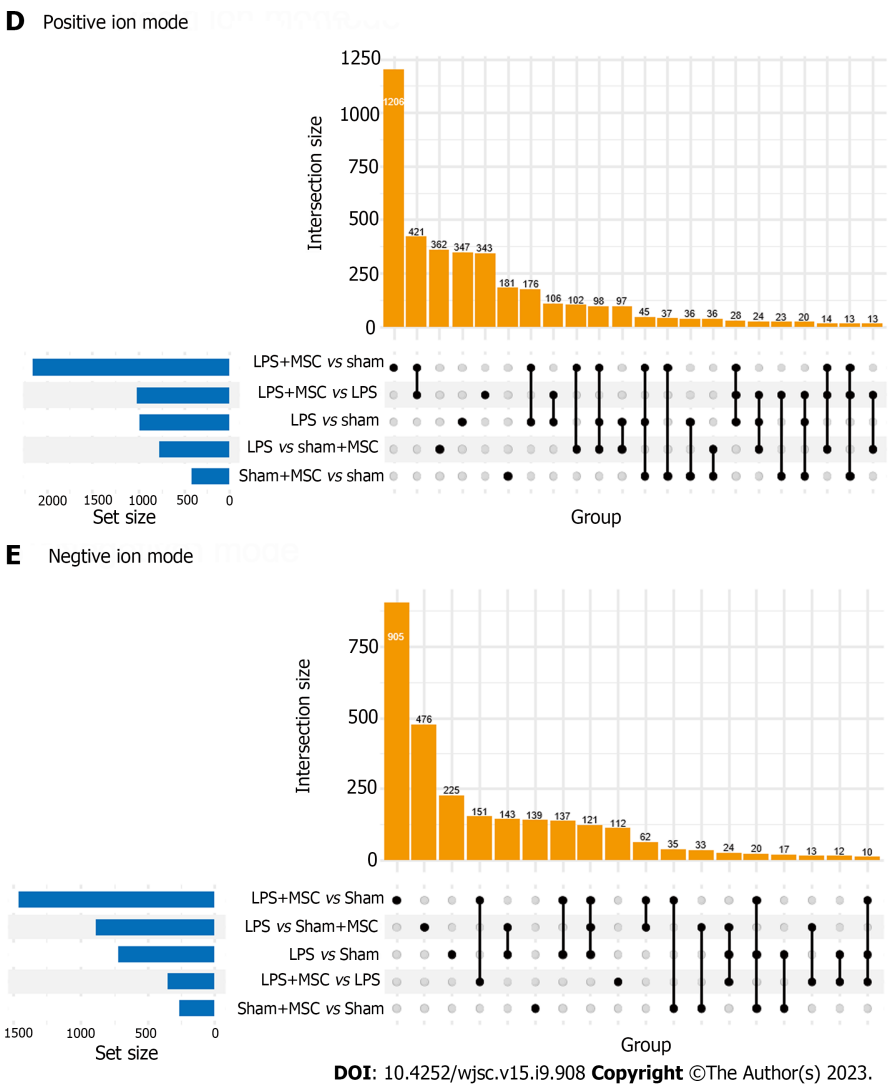

DOI: 10.4252/wjsc.v15.i9.908 **Copyright** ©The Author(s) 2023.

Figure 7 Metabolomics for the lung (*n* = 6). A: Base peak chromatogram in positive/negative mode; B and C: The Partial Least Squares-Discriminant Analysis was used to distinguish metabolite differences between groups in positive/negative mode; D and E: Upset Venn diagrams were used to count the number of common and unique differential metabolites in different groups. The bar chart at the bottom left represents the total number of differential metabolites between two groups. The bar chart above shows common metabolites. The results are based on mass spectrum analysis data. LPS: Lipopolysaccharide; MSC: Mesenchymal stem cell.

between the BALF microflora and lung tissue metabolites using the O2PLS method. *Haemophilus* has a pivotal role in improving ALI mice by HUC-MSCs. One study reported that non-typeable *Haemophilus influenzae* induces neutrophilic inflammation in severe asthma[57]. Moreover, Yue *et al*[58] found that autophagy can combat the inflammation caused by *Haemophilus parasuis*, acting as a cellular defense mechanism. Similarly, KEGG enrichment results of the high-impact metabolites predicted by O2PLS suggested that autophagy-related pathways may play a critical role in HUC-MSC treatment in ALI mice. The exploration of lung metabolites contributes to the biological mechanism and biomarker discovery of HUM-MSCs treatment in ALI.

Naturally, this study only examined the correlation between microarray and metabolomics in the lung and gut and cannot have conclusive evidence to confirm that the lung-gut axis microbiota is a crucial factor behind the ability of HUC-MSCs to improve ALI. Animal and clinical studies are necessary to validate the role of gut and lung microorganisms in the improvement of ALI by HUC-MSCs. As depicted in Figure 10, this research showcases the crucial involvement of the lung-intestinal axis in safeguarding the lungs and intestines of ALI rats treated with HUC-MSCs, highlighting the interconnectedness of the lung-intestinal microbiota and metabolites.

CONCLUSION

This study showed that HUM-MSC treatment of ALI improved the edema, tissue injury, and endothelial barrier function of the lung; upregulated the VE-cadherin, ZO-1, and occludin levels in the lung; and inhibited the inflammatory cytokine expression levels in the serum and lung. Moreover, HUM-MSC treatment of ALI attenuated the expression of the TLR4/Myd88/NF-κB signaling pathway in the lung tissue. In addition, HUM-MSC treatment of ALI mice improved ileal histopathological damage, reduced the levels of inflammatory factors, promoted ZO-1, claudin-1, and occludin protein

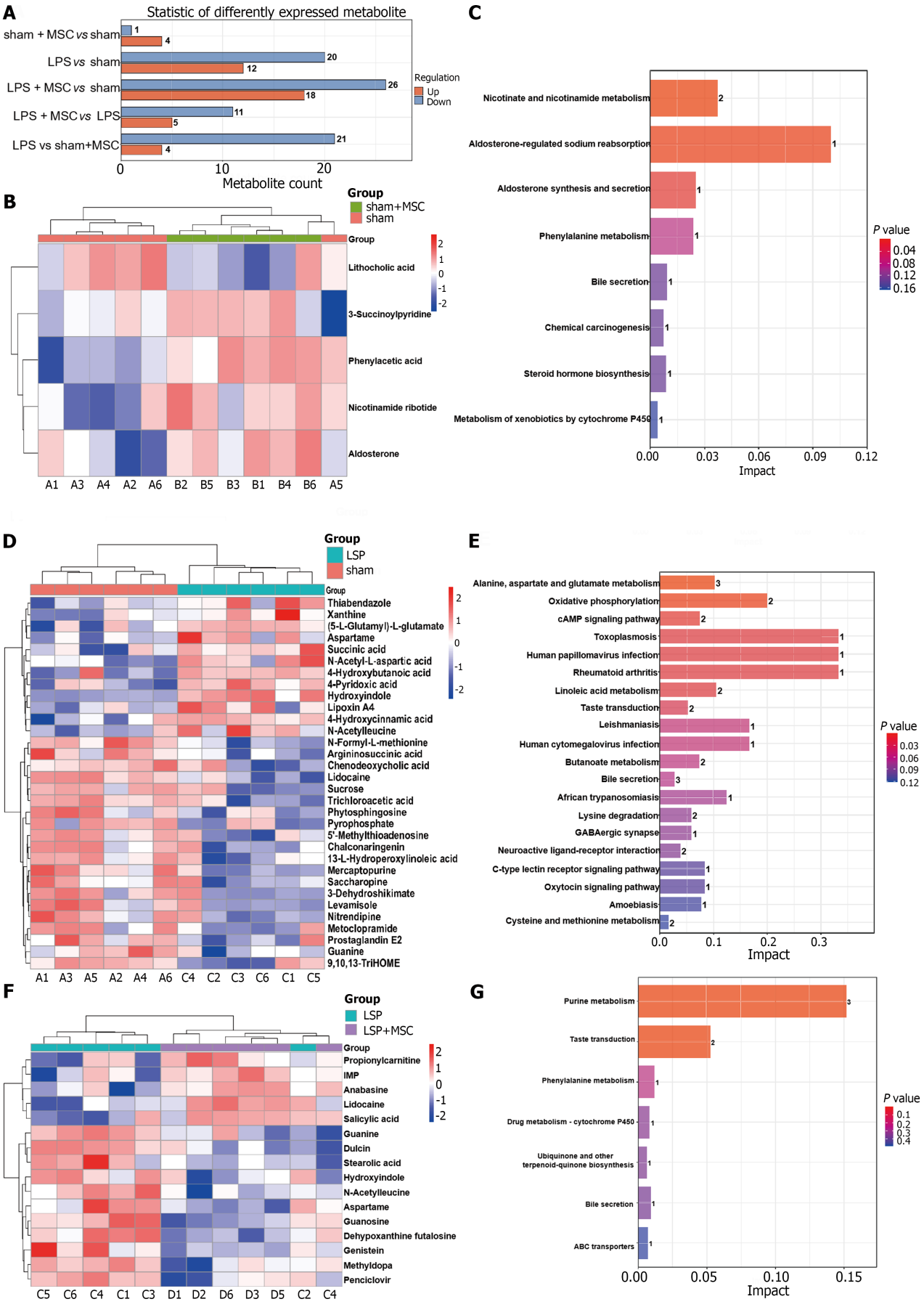

DOI: 10.4252/wjsc.v15.i9.908 **Copyright** ©The Author(s) 2023.

Figure 8 Screening of differently expressed metabolites in acute lung injury mice treated with human umbilical cord mesenchymal stem

cells (*n* = 6). A: Statistic of differently expressed metabolites under liquid chromatography-tandem mass spectrometry mode; B: Heatmaps of sham + mesenchymal stem cells (MSCs) group *vs* sham group; C: Kyoto Encyclopedia of Genes and Genomes (KEGG) pathways enriched by differently expressed metabolites of sham + MSC group *vs* sham group; D: The lipopolysaccharide (LPS) group *vs* sham group were used to analyze and display differently expressed metabolites; E: KEGG pathway enriched by differently expressed metabolites of LPS group *vs* sham group; F: Heatmaps of LPS group *vs* LPS + MSC group; G: KEGG pathways enriched by differently expressed metabolites of sham + MSC group *vs* sham group. LPS: Lipopolysaccharide; MSC: Mesenchymal stem cell.

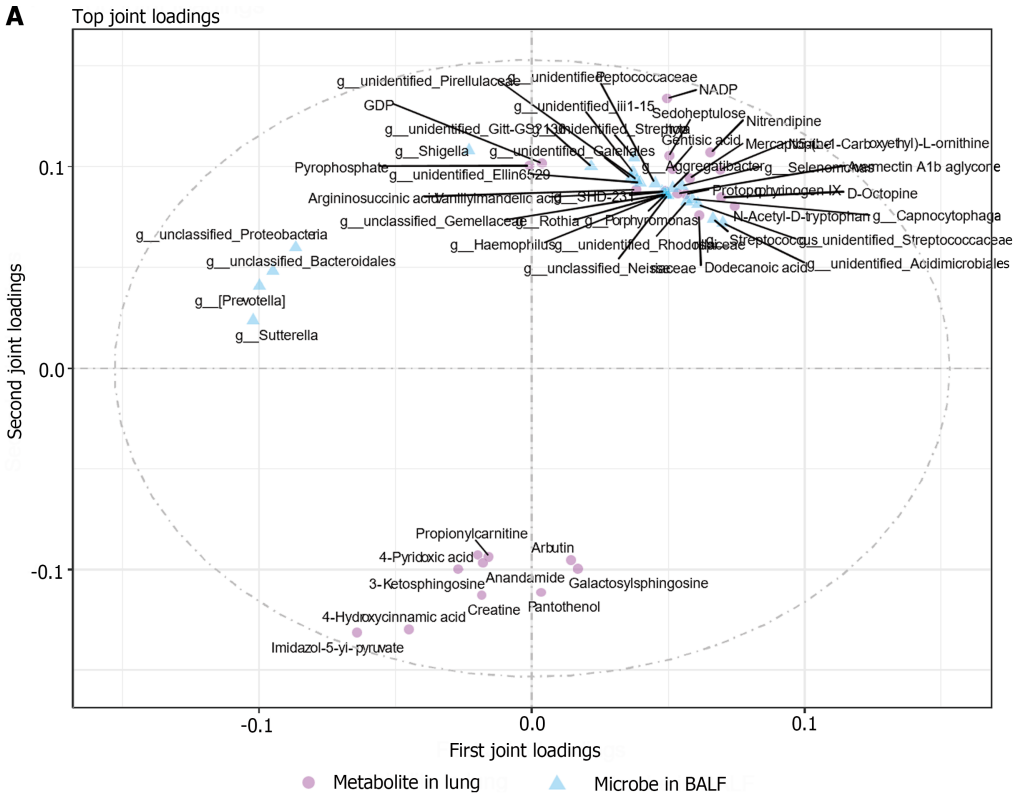

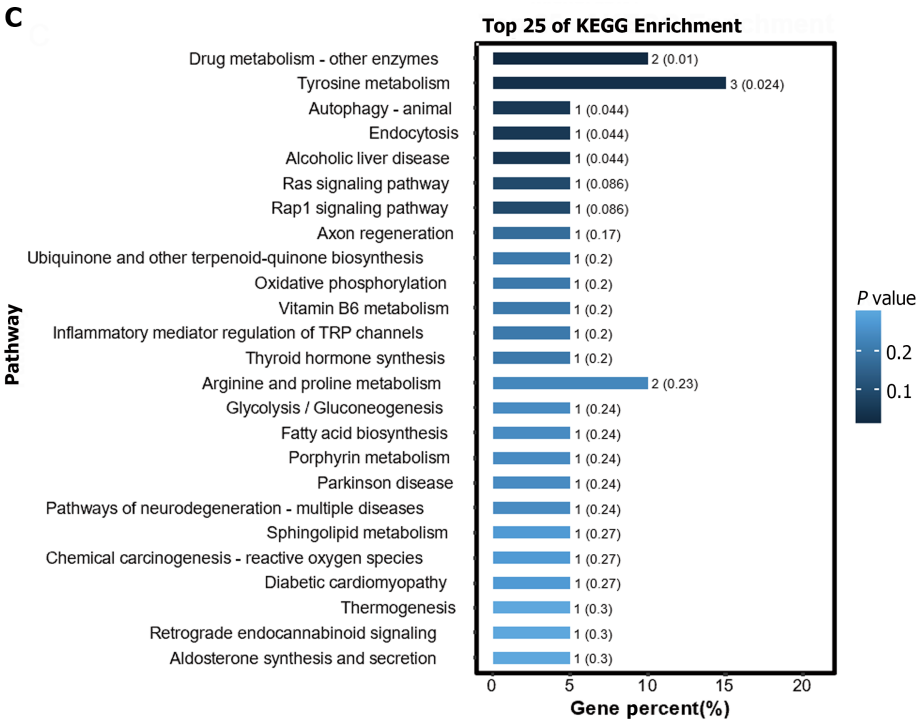

DOI: 10.4252/wjsc.v15.i9.908 **Copyright** ©The Author(s) 2023.

Figure 9 Extent of correlation between lung metabolites and bronchoalveolar lavage fluid microflorae. A: Top 25 lung metabolites and top 25 bronchoalveolar lavage fluid (BALF) microflorae were analyzed by the two-way Orthogonal Partial Least Squares analysis. A larger absolute value in a coordinate indicates a greater degree of association. Circles represent metabolites in lung tissues and squares represent microflora in BALF; B: The number of lung metabolites which were related with BALF microflorae; C: Kyoto Encyclopedia of Genes and Genomes enrichment analysis of top 25 BALF microflorae with strong association. KEGG: Kyoto Encyclopedia of Genes and Genomes; BALF: Bronchoalveolar lavage fluid.

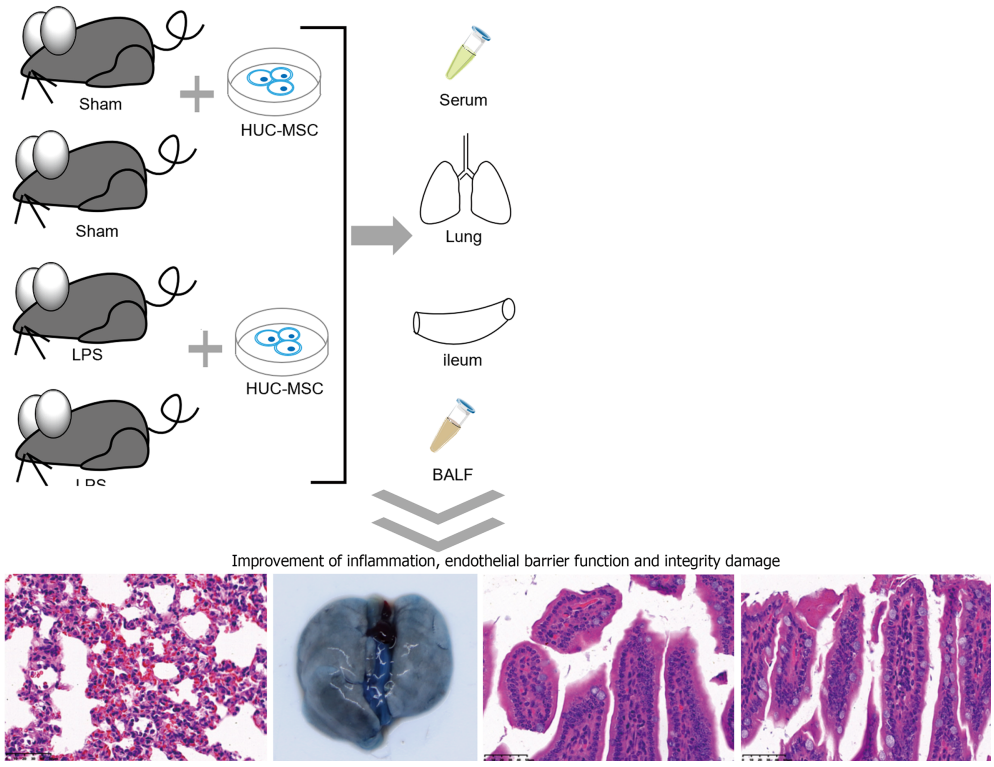

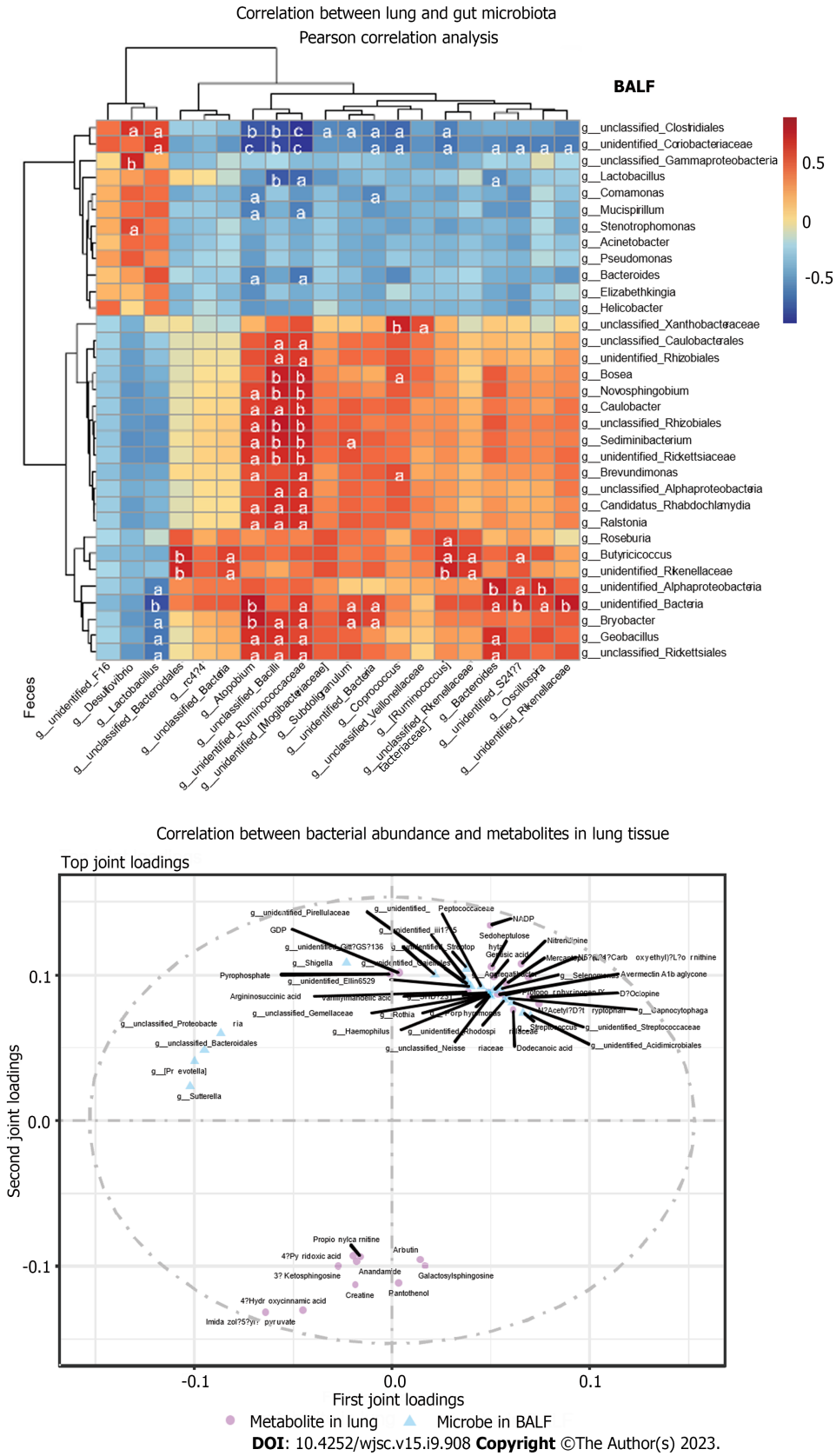

DOI: 10.4252/wjsc.v15.i9.908 **Copyright** ©The Author(s) 2023.

Figure 10 Graphical abstract. LPS: Lipopolysaccharide; MSC: Mesenchymal stem cell; BALF: Bronchoalveolar lavage fluid.

expression, and decreased EUB338 counts in the lung and ileum. In particular, this study found that the gut and lung microflora and metabolites were significantly different between ALI mice untreated and treated with HUM-MSCs. There was a correlation between the abundances of the gut and lung microflora. *Lactobacillus*, *Bacteroides*, and *unidentifiedden-tified_Rikenellaceae* genera are potential biomarkers for evaluating the treatment efficacy of HUC-MSCs. Additionally, this study contributes to the biological mechanism and biomarker discovery of HUM-MSC treatment of ALI by the combined

analysis of lung tissue metabolomics and microbiota, providing a scientific basis for the biological mechanism and clinical application of HUC-MSCs and new ideas for the development of therapeutic strategies for ALI.

ARTICLE HIGHLIGHTS

Research background

Acute lung injury (ALI) has high morbidity and mortality rates and needs effective treatment. Research has found that the gut microbiota improves lung injury through the lung-gut axis. Human umbilical cord mesenchymal cells (HUC-MSCs) can improve ALI.

Research motivation

Although HUC-MSCs can improve ALI, their biological mechanism of action is not yet clear.

Research objectives

To explore changes in the microbiota in the lung-gut axis and the relationship with HUC-MSC treatment.

Research methods

C57BL/6 mice were used to establish an ALI animal model by intraperitoneal injections of lipopolysaccharide. Wright's staining, ELISA, hematoxylin-eosin staining, Evans blue dye leakage assay, immunohistochemistry, fluorescence *in situ* hybridization, and western blot were used to observe the improvement of ALI mice by HUC-MSCs. High-throughput 16S rDNA sequencing was used to observe the microbiota homeostases in the lung-gut axis. The non-targeted metabolomics was used to explore changes in lung tissue metabolites.

Research results

HUC-MSCs ameliorated histopathological damage in the lung and ileum of ALI mice. HUC-MSC treatment improved inflammation, endothelial barrier integrity, and bacterial translocation in the lungs and ileum of ALI mice. HUC-MSCs regulated lung-gut microbiota homeostasis. HUC-MSC treatment regulated the metabolic profile in the lung and ileum of ALI mice.

Research conclusions

This study shows the improvement of changes in the lung and ileum of ALI mice by HUC-MSCs, and suggests a correlation between HUM-MSC-improved ALI and gut and lung microbiota homeostases.

Research perspectives

This study explores the biological mechanism of HUC-MSCs in improving ALI from the perspective of the correlation between the microbiota in the lung-gut axis and lung tissue metabolites, providing a research basis for HUC-MSC treatment.

FOOTNOTES

Author contributions: Cui EH, Lv L, and Wang B conceived and designed the research; Lv L, Li LQ, and Lu HD acquired the data; Cui EH, Li LQ, and Hua F analyzed and interpreted the data; Lv L, Lu HD, Chen WY, and Chen N performed statistical analysis; Cui EH and Wang B obtained the funding; Lv L and Cui EH drafted the manuscript; Cui EH, Wang B, and Hua F revised the manuscript for important intellectual content; and all authors approved the final version of the article.

Supported by the Key Research and Development Project of Science and Technology Department of Zhejiang Province, No. 2019C03041.

Institutional review board statement: The study was reviewed and approved by the Animal Experimentation Ethics Committee of Zhejiang Eyong Pharmaceutical Research and Development Center (License No. SYXK(Zhe)2021-0033).

Institutional animal care and use committee statement: All animal experiments conformed to the internationally accepted principles for the care and use of laboratory animals (Approval No. ZJEY-20220721-02).

Conflict-of-interest statement: All the authors report no relevant conflicts of interest for this article.

Data sharing statement: No additional data are available.

ARRIVE guidelines statement: The authors have read the ARRIVE guidelines, and the manuscript was prepared and revised according to the ARRIVE guidelines.

Open-Access: This article is an open-access article that was selected by an in-house editor and fully peer-reviewed by external reviewers. It is distributed in accordance with the Creative Commons Attribution NonCommercial (CC BY-NC 4.0) license, which permits others to

distribute, remix, adapt, build upon this work non-commercially, and license their derivative works on different terms, provided the original work is properly cited and the use is non-commercial. See: https://creativecommons.org/Licenses/by-nc/4.0/

Country/Territory of origin: China

ORCID number: En-Hai Cui 0000-0002-8808-8793.

S-Editor: Wang JJ
L-Editor: Wang TQ
P-Editor: Cai YX

REFERENCES

1 **Xia L**, Zhang C, Lv N, Liang Z, Ma T, Cheng H, Xia Y, Shi L. AdMSC-derived exosomes alleviate acute lung injury *via* transferring mitochondrial component to improve homeostasis of alveolar macrophages. *Theranostics* 2022; **12**: 2928-2947 [PMID: 35401830 DOI: 10.7150/thno.69533]

2 **Palikova YA**, Palikov VA, Novikova NI, Slashcheva GA, Rasskazova EA, Tukhovskaya EA, Danilkovich AV, Dyachenko IA, Belogurov AA Jr, Kudriaeva AA, Bugrimov DY, Krasnorutskaya ON, Murashev AN. Derinat(®) has an immunomodulatory and anti-inflammatory effect on the model of acute lung injury in male SD rats. *Front Pharmacol* 2022; **13**: 1111340 [PMID: 36642990 DOI: 10.3389/fphar.2022.1111340]

3 **Li J**, Deng SH, Li J, Li L, Zhang F, Zou Y, Wu DM, Xu Y. Obacunone alleviates ferroptosis during lipopolysaccharide-induced acute lung injury by upregulating Nrf2-dependent antioxidant responses. *Cell Mol Biol Lett* 2022; **27**: 29 [PMID: 35305560 DOI: 10.1186/s11658-022-00318-8]

4 **Fan E**, Brodie D, Slutsky AS. Acute Respiratory Distress Syndrome: Advances in Diagnosis and Treatment. *JAMA* 2018; **319**: 698-710 [PMID: 29466596 DOI: 10.1001/jama.2017.21907]

5 **Hou L**, Zhang J, Liu Y, Fang H, Liao L, Wang Z, Yuan J, Wang X, Sun J, Tang B, Chen H, Ye P, Ding Z, Lu H, Wang Y. MitoQ alleviates LPS-mediated acute lung injury through regulating Nrf2/Drp1 pathway. *Free Radic Biol Med* 2021; **165**: 219-228 [PMID: 33539948 DOI: 10.1016/j.freeradbiomed.2021.01.045]

6 **Ju M**, Liu B, He H, Gu Z, Liu Y, Su Y, Zhu D, Cang J, Luo Z. MicroRNA-27a alleviates LPS-induced acute lung injury in mice *via* inhibiting inflammation and apoptosis through modulating TLR4/MyD88/NF-κB pathway. *Cell Cycle* 2018; **17**: 2001-2018 [PMID: 30231673 DOI: 10.1080/15384101.2018.1509635]

7 **Yang C**, Song C, Liu Y, Qu J, Li H, Xiao W, Kong L, Ge H, Sun Y, Lv W. Re-Du-Ning injection ameliorates LPS-induced lung injury through inhibiting neutrophil extracellular traps formation. *Phytomedicine* 2021; **90**: 153635 [PMID: 34229173 DOI: 10.1016/j.phymed.2021.153635]

8 **Tang J**, Xu L, Zeng Y, Gong F. Effect of gut microbiota on LPS-induced acute lung injury by regulating the TLR4/NF-kB signaling pathway. *Int Immunopharmacol* 2021; **91**: 107272 [PMID: 33360370 DOI: 10.1016/j.intimp.2020.107272]

9 **Dickson RP**, Schultz MJ, van der Poll T, Schouten LR, Falkowski NR, Luth JE, Sjoding MW, Brown CA, Chanderraj R, Huffnagle GB, Bos LDJ; Biomarker Analysis in Septic ICU Patients (BASIC) Consortium. Lung Microbiota Predict Clinical Outcomes in Critically Ill Patients. *Am J Respir Crit Care Med* 2020; **201**: 555-563 [PMID: 31973575 DOI: 10.1164/rccm.201907-1487OC]

10 **Jin C**, Chen J, Gu J, Zhang W. Gut-lymph-lung pathway mediates sepsis-induced acute lung injury. *Chin Med J (Engl)* 2020; **133**: 2212-2218 [PMID: 32858588 DOI: 10.1097/CM9.0000000000000928]

11 **Yoon YM**, Hrusch CL, Fei N, Barrón GM, Mills KAM, Hollinger MK, Velez TE, Leone VA, Chang EB, Sperling AI. Gut microbiota modulates bleomycin-induced acute lung injury response in mice. *Respir Res* 2022; **23**: 337 [PMID: 36496380 DOI: 10.1186/s12931-022-02264-7]

12 **Hashimoto Y**, Eguchi A, Wei Y, Shinno-Hashimoto H, Fujita Y, Ishima T, Chang L, Mori C, Suzuki T, Hashimoto K. Antibiotic-induced microbiome depletion improves LPS-induced acute lung injury *via* gut-lung axis. *Life Sci* 2022; **307**: 120885 [PMID: 35981631 DOI: 10.1016/j.lfs.2022.120885]

13 **Yeoh YK**, Zuo T, Lui GC, Zhang F, Liu Q, Li AY, Chung AC, Cheung CP, Tso EY, Fung KS, Chan V, Ling L, Joynt G, Hui DS, Chow KM, Ng SSS, Li TC, Ng RW, Yip TC, Wong GL, Chan FK, Wong CK, Chan PK, Ng SC. Gut microbiota composition reflects disease severity and dysfunctional immune responses in patients with COVID-19. *Gut* 2021; **70**: 698-706 [PMID: 33431578 DOI: 10.1136/gutjnl-2020-323020]

14 **Tang Q**, Liu R, Chu G, Wang Y, Cui H, Zhang T, Bi K, Gao P, Song Z, Li Q. A Comprehensive Analysis of Microflora and Metabolites in the Development of Ulcerative Colitis into Colorectal Cancer Based on the Lung-Gut Correlation Theory. *Molecules* 2022; **27** [PMID: 36144573 DOI: 10.3390/molecules27185838]

15 **Samsonraj RM**, Raghunath M, Nurcombe V, Hui JH, van Wijnen AJ, Cool SM. Concise Review: Multifaceted Characterization of Human Mesenchymal Stem Cells for Use in Regenerative Medicine. *Stem Cells Transl Med* 2017; **6**: 2173-2185 [PMID: 29076267 DOI: 10.1002/sctm.17-0129]

16 **Ding DC**, Shyu WC, Lin SZ. Mesenchymal stem cells. *Cell Transplant* 2011; **20**: 5-14 [PMID: 21396235 DOI: 10.3727/096368910X]

17 **Xu Y**, Zhu J, Feng B, Lin F, Zhou J, Liu J, Shi X, Lu X, Pan Q, Yu J, Zhang Y, Li L, Cao H. Immunosuppressive effect of mesenchymal stem cells on lung and gut CD8(+) T cells in lipopolysaccharide-induced acute lung injury in mice. *Cell Prolif* 2021; **54**: e13028 [PMID: 33738881 DOI: 10.1111/cpr.13028]

18 **Kakabadze Z**, Kipshidze N, Paresishvili T, Vadachkoria Z, Chakhunashvili D. Human Placental Mesenchymal Stem Cells for the Treatment of ARDS in Rat. *Stem Cells Int* 2022; **2022**: 8418509 [PMID: 35756754 DOI: 10.1155/2022/8418509]

19 **Ahn SY**, Chang YS, Kim JH, Sung SI, Park WS. Two-Year Follow-Up Outcomes of Premature Infants Enrolled in the Phase I Trial of Mesenchymal Stem Cells Transplantation for Bronchopulmonary Dysplasia. *J Pediatr* 2017; **185**: 49-54.e2 [PMID: 28341525 DOI: 10.1016/j.jpeds.2017.02.061]

20 **Tu C**, Wang Z, Xiang E, Zhang Q, Zhang Y, Wu P, Li C, Wu D. Human Umbilical Cord Mesenchymal Stem Cells Promote Macrophage PD-L1 Expression and Attenuate Acute Lung Injury in Mice. *Curr Stem Cell Res Ther* 2022; **17**: 564-575 [PMID: 35086457 DOI: 10.2174/1574888X17666220127110332]

21 **Choi SM**, Mo Y, Bang JY, Ko YG, Ahn YH, Kim HY, Koh J, Yim JJ, Kang HR. Classical monocyte-derived macrophages as therapeutic targets of umbilical cord mesenchymal stem cells: comparison of intratracheal and intravenous administration in a mouse model of pulmonary fibrosis. *Respir Res* 2023; **24**: 68 [PMID: 36870972 DOI: 10.1186/s12931-023-02357-x]

22 **Liu A**, Wang X, Liang X, Wang W, Li C, Qian J, Zhang X. Human umbilical cord mesenchymal stem cells regulate immunoglobulin a secretion and remodel the diversification of intestinal microbiota to improve colitis. *Front Cell Infect Microbiol* 2022; **12**: 960208 [PMID: 36118029 DOI: 10.3389/fcimb.2022.960208]

23 **Luo L**, Chen Q, Yang L, Zhang Z, Xu J, Gou D. MSCs Therapy Reverse the Gut Microbiota in Hypoxia-Induced Pulmonary Hypertension Mice. *Front Physiol* 2021; **12**: 712139 [PMID: 34531759 DOI: 10.3389/fphys.2021.712139]

24 **Wu KH**, Li JP, Chao WR, Lee YJ, Yang SF, Cheng CC, Chao YH. Immunomodulation *via* MyD88-NFκB Signaling Pathway from Human Umbilical Cord-Derived Mesenchymal Stem Cells in Acute Lung Injury. *Int J Mol Sci* 2022; **23** [PMID: 35628107 DOI: 10.3390/ijms23105295]

25 **Li Y**, Xu J, Shi W, Chen C, Shao Y, Zhu L, Lu W, Han X. Mesenchymal stromal cell treatment prevents H9N2 avian influenza virus-induced acute lung injury in mice. *Stem Cell Res Ther* 2016; **7**: 159 [PMID: 27793190 DOI: 10.1186/s13287-016-0395-z]

26 **Hao X**, Wei H. LncRNA H19 alleviates sepsis-induced acute lung injury by regulating the miR-107/TGFBR3 axis. *BMC Pulm Med* 2022; **22**: 371 [PMID: 36180862 DOI: 10.1186/s12890-022-02091-y]

27 **Yang J**, Watkins D, Chen CL, Bhushan B, Zhou Y, Besner GE. Heparin-binding epidermal growth factor-like growth factor and mesenchymal stem cells act synergistically to prevent experimental necrotizing enterocolitis. *J Am Coll Surg* 2012; **215**: 534-545 [PMID: 22819639 DOI: 10.1016/j.jamcollsurg.2012.05.037]

28 **Jin S**, Ding X, Yang C, Li W, Deng M, Liao H, Lv X, Pitt BR, Billiar TR, Zhang LM, Li Q. Mechanical Ventilation Exacerbates Poly (I:C) Induced Acute Lung Injury: Central Role for Caspase-11 and Gut-Lung Axis. *Front Immunol* 2021; **12**: 693874 [PMID: 34349759 DOI: 10.3389/fimmu.2021.693874]

29 **Peng J**, Li J, Huang J, Xu P, Huang H, Liu Y, Yu L, Yang Y, Zhou B, Jiang H, Chen K, Dang Y, Zhang Y, Luo C, Li G. p300/CBP inhibitor A-485 alleviates acute liver injury by regulating macrophage activation and polarization. *Theranostics* 2019; **9**: 8344-8361 [PMID: 31754401 DOI: 10.7150/thno.30707]

30 **Liu X**, Song Y, Li R. The use of combined PCR, fluorescence in situ hybridisation and immunohistochemical staining to diagnose mucormycosis from formalin-fixed paraffin-embedded tissues. *Mycoses* 2021; **64**: 1460-1470 [PMID: 34674327 DOI: 10.1111/myc.13382]

31 **Yi Q**, Liu J, Zhang Y, Qiao H, Chen F, Zhang S, Guan W. Anethole Attenuates Enterotoxigenic Escherichia coli-Induced Intestinal Barrier Disruption and Intestinal Inflammation *via* Modification of TLR Signaling and Intestinal Microbiota. *Front Microbiol* 2021; **12**: 647242 [PMID: 33841372 DOI: 10.3389/fmicb.2021.647242]

32 **Lyu F**, Han F, Ge C, Mao W, Chen L, Hu H, Chen G, Lang Q, Fang C. Omicstudio: A composable bioinformatics cloud platform with real-time feedback that can generate high-quality graphs for publication. *iMeta* 2023; **2** [DOI: 10.1002/imt2.85]

33 **Wishart DS**, Guo A, Oler E, Wang F, Anjum A, Peters H, Dizon R, Sayeeda Z, Tian S, Lee BL, Berjanskii M, Mah R, Yamamoto M, Jovel J, Torres-Calzada C, Hiebert-Giesbrecht M, Lui VW, Varshavi D, Allen D, Arndt D, Khetarpal N, Sivakumaran A, Harford K, Sanford S, Yee K, Cao X, Budinski Z, Liigand J, Zhang L, Zheng J, Mandal R, Karu N, Dambrova M, Schiöth HB, Greiner R, Gautam V. HMDB 5.0: the Human Metabolome Database for 2022. *Nucleic Acids Res* 2022; **50**: D622-D631 [PMID: 34986597 DOI: 10.1093/nar/gkab1062]

34 **Kanehisa M**, Furumichi M, Sato Y, Kawashima M, Ishiguro-Watanabe M. KEGG for taxonomy-based analysis of pathways and genomes. *Nucleic Acids Res* 2023; **51**: D587-D592 [PMID: 36300620 DOI: 10.1093/nar/gkac963]

35 **Huang Y**, Wu Q, Tam PKH. Immunomodulatory Mechanisms of Mesenchymal Stem Cells and Their Potential Clinical Applications. *Int J Mol Sci* 2022; **23** [PMID: 36077421 DOI: 10.3390/ijms231710023]

36 **Jerkic M**, Szaszi K, Laffey JG, Rotstein O, Zhang H. Key Role of Mesenchymal Stromal Cell Interaction with Macrophages in Promoting Repair of Lung Injury. *Int J Mol Sci* 2023; **24** [PMID: 36834784 DOI: 10.3390/ijms24043376]

37 **Wang Y**, Zhang Y, Lu B, Xi J, Ocansey DKW, Mao F, Hao D, Yan Y. hucMSC-Ex Alleviates IBD-Associated Intestinal Fibrosis by Inhibiting ERK Phosphorylation in Intestinal Fibroblasts. *Stem Cells Int* 2023; **2023**: 2828981 [PMID: 36845967 DOI: 10.1155/2023/2828981]

38 **Soe HJ**, Khan AM, Manikam R, Samudi Raju C, Vanhoutte P, Sekaran SD. High dengue virus load differentially modulates human microvascular endothelial barrier function during early infection. *J Gen Virol* 2017; **98**: 2993-3007 [PMID: 29182510 DOI: 10.1099/jgv.0.000981]

39 **Jiao Y**, Zhang T, Zhang C, Ji H, Tong X, Xia R, Wang W, Ma Z, Shi X. Exosomal miR-30d-5p of neutrophils induces M1 macrophage polarization and primes macrophage pyroptosis in sepsis-related acute lung injury. *Crit Care* 2021; **25**: 356 [PMID: 34641966 DOI: 10.1186/s13054-021-03775-3]

40 **Kao TI**, Chen PJ, Wang YH, Tseng HH, Chang SH, Wu TS, Yang SH, Lee YT, Hwang TL. Bletinib ameliorates neutrophilic inflammation and lung injury by inhibiting Src family kinase phosphorylation and activity. *Br J Pharmacol* 2021; **178**: 4069-4084 [PMID: 34131920 DOI: 10.1111/bph.15597]

41 **Chen DQ**, Shen MJ, Wang H, Li Y, Tang AL, Li S, Xiong MC, Guo Y, Zhang GQ. Sirt3 Maintains Microvascular Endothelial Adherens Junction Integrity to Alleviate Sepsis-Induced Lung Inflammation by Modulating the Interaction of VE-Cadherin and β-Catenin. *Oxid Med Cell Longev* 2021; **2021**: 8978795 [PMID: 34630854 DOI: 10.1155/2021/8978795]

42 **Botros L**, Pronk MCA, Juschten J, Liddle J, Morsing SKH, van Buul JD, Bates RH, Tuinman PR, van Bezu JSM, Huveneers S, Bogaard HJ, van Hinsbergh VWM, Hordijk PL, Aman J. Bosutinib prevents vascular leakage by reducing focal adhesion turnover and reinforcing junctional integrity. *J Cell Sci* 2020; **133** [PMID: 32198280 DOI: 10.1242/jcs.240077]

43 **Wang YW**, Wu YH, Zhang JZ, Tang JH, Fan RP, Li F, Yu BY, Kou JP, Zhang YY. Ruscogenin attenuates particulate matter-induced acute lung injury in mice *via* protecting pulmonary endothelial barrier and inhibiting TLR4 signaling pathway. *Acta Pharmacol Sin* 2021; **42**: 726-734 [PMID: 32855531 DOI: 10.1038/s41401-020-00502-6]

44 **Zhang L**, Li Q, Liu W, Liu Z, Shen H, Zhao M. Mesenchymal Stem Cells Alleviate Acute Lung Injury and Inflammatory Responses Induced by Paraquat Poisoning. *Med Sci Monit* 2019; **25**: 2623-2632 [PMID: 30967525 DOI: 10.12659/MSM.915804]

45 **Płóciennikowska A**, Hromada-Judycka A, Borzęcka K, Kwiatkowska K. Co-operation of TLR4 and raft proteins in LPS-induced pro-inflammatory signaling. *Cell Mol Life Sci* 2015; **72**: 557-581 [PMID: 25332099 DOI: 10.1007/s00018-014-1762-5]

46 **Chai L**, Wang Q, Si C, Gao W, Zhang L. Potential Association Between Changes in Microbiota Level and Lung Diseases: A Meta-Analysis. *Front Med (Lausanne)* 2021; **8**: 723635 [PMID: 35096850 DOI: 10.3389/fmed.2021.723635]

47 **Brooke JS**. Stenotrophomonas maltophilia: an emerging global opportunistic pathogen. *Clin Microbiol Rev* 2012; **25**: 2-41 [PMID: 22232370 DOI: 10.1128/CMR.00019-11]

48 **Ryan MP**, Sevjahova L, Gorman R, White S. The Emergence of the Genus Comamonas as Important Opportunistic Pathogens. *Pathogens* 2022; **11** [PMID: 36145464 DOI: 10.3390/pathogens11091032]

49 **Lin JN**, Lai CH, Yang CH, Huang YH. Elizabethkingia Infections in Humans: From Genomics to Clinics. *Microorganisms* 2019; **7** [PMID: 31466280 DOI: 10.3390/microorganisms7090295]

50 **Liu Z**, Xu W. Neutrophil and Macrophage Response in Acinetobacter Baumannii Infection and Their Relationship to Lung Injury. *Front Cell Infect Microbiol* 2022; **12**: 890511 [PMID: 35873147 DOI: 10.3389/fcimb.2022.890511]

51 **Chen YR**, Zheng HM, Zhang GX, Chen FL, Chen LD, Yang ZC. High Oscillospira abundance indicates constipation and low BMI in the Guangdong Gut Microbiome Project. *Sci Rep* 2020; **10**: 9364 [PMID: 32518316 DOI: 10.1038/s41598-020-66369-z]

52 **Keshavarzian A**, Green SJ, Engen PA, Voigt RM, Naqib A, Forsyth CB, Mutlu E, Shannon KM. Colonic bacterial composition in Parkinson's disease. *Mov Disord* 2015; **30**: 1351-1360 [PMID: 26179554 DOI: 10.1002/mds.26307]

53 **Herp S**, Durai Raj AC, Salvado Silva M, Woelfel S, Stecher B. The human symbiont Mucispirillum schaedleri: causality in health and disease. *Med Microbiol Immunol* 2021; **210**: 173-179 [PMID: 34021796 DOI: 10.1007/s00430-021-00702-9]

54 **Huang L**, Wang J, Kong L, Wang X, Li Q, Zhang L, Shi J, Duan J, Mu H. ROS-responsive hyaluronic acid hydrogel for targeted delivery of probiotics to relieve colitis. *Int J Biol Macromol* 2022; **222**: 1476-1486 [PMID: 36195227 DOI: 10.1016/j.ijbiomac.2022.09.247]

55 **Johnstone J**, Meade M, Lauzier F, Marshall J, Duan E, Dionne J, Arabi YM, Heels-Ansdell D, Thabane L, Lamarche D, Surette M, Zytaruk N, Mehta S, Dodek P, McIntyre L, English S, Rochwerg B, Karachi T, Henderson W, Wood G, Ovakim D, Herridge M, Granton J, Wilcox ME, Goffi A, Stelfox HT, Niven D, Muscedere J, Lamontagne F, D'Aragon F, St-Arnaud C, Ball I, Nagpal D, Girard M, Aslanian P, Charbonney E, Williamson D, Sligl W, Friedrich J, Adhikari NK, Marquis F, Archambault P, Khwaja K, Kristof A, Kutsogiannis J, Zarychanski R, Paunovic B, Reeve B, Lellouche F, Hosek P, Tsang J, Binnie A, Trop S, Loubani O, Hall R, Cirone R, Reynolds S, Lysecki P, Golan E, Cartin-Ceba R, Taylor R, Cook D; Prevention of Severe Pneumonia and Endotracheal Colonization Trial (PROSPECT) Investigators and the Canadian Critical Care Trials Group. Effect of Probiotics on Incident Ventilator-Associated Pneumonia in Critically Ill Patients: A Randomized Clinical Trial. *JAMA* 2021; **326**: 1024-1033 [PMID: 34546300 DOI: 10.1001/jama.2021.13355]

56 **Gadaleta RM**, van Mil SW, Oldenburg B, Siersema PD, Klomp LW, van Erpecum KJ. Bile acids and their nuclear receptor FXR: Relevance for hepatobiliary and gastrointestinal disease. *Biochim Biophys Acta* 2010; **1801**: 683-692 [PMID: 20399894 DOI: 10.1016/j.bbalip.2010.04.006]

57 **Ackland J**, Barber C, Heinson A, Azim A, Cleary DW, Christodoulides M, Kurukulaaratchy RJ, Howarth P, Wilkinson TMA, Staples KJ; WATCH study investigators. Nontypeable Haemophilus influenzae infection of pulmonary macrophages drives neutrophilic inflammation in severe asthma. *Allergy* 2022; **77**: 2961-2973 [PMID: 35570583 DOI: 10.1111/all.15375]

58 **Yue C**, Li J, Jin H, Hua K, Zhou W, Wang Y, Cheng G, Liu D, Xu L, Chen Y, Zeng Y. Autophagy Is a Defense Mechanism Inhibiting Invasion and Inflammation During High-Virulent Haemophilus parasuis Infection in PK-15 Cells. *Front Cell Infect Microbiol* 2019; **9**: 93 [PMID: 31106159 DOI: 10.3389/fcimb.2019.00093]

Published by **Baishideng Publishing Group Inc**
7041 Koll Center Parkway, Suite 160, Pleasanton, CA 94566, USA
Telephone: +1-925-3991568
E-mail: bpgoffice@wjgnet.com
Help Desk: https://www.f6publishing.com/helpdesk
https://www.wjgnet.com

© 2023 Baishideng Publishing Group Inc. All rights reserved.